Polyamine receptors containing anthracene as fluorescent probes for ketoprofen in H_2O/EtOH solution

Giammarco Maria Romano, Liviana Mummolo, Matteo Savastano, Paola Paoli, Patrizia Rossi, Luca Prodi, Andrea Bencini

Electronic Supplementary Information (ESI)

Synthesis of L1 and L2

Ligands **L1** and **L2** were synthetized as summarized in Scheme S1.

N1,N3-bis(9-anthrylmethyl)diethylenetriamine (L1). A solution of 9-anthraldehyde (0.8 g, 3.88 mmol) in EtOH/CH_3CN 50:50 v/v (50 mL) was added dropwise to a solution of diethylenetriamine (0.2 g, 1.9 mmol) in a mixture solvent of EtOH/CH_3CN 50:50 v/v (50 mL). The solution was stirred a room temperature for 60 h. the solution was then concentrated by evaporation. The resulting oil was dissolved in EtOH (100 mL) and stirred with $NaBH_4$ (0.76 g, 20 mmol) at 60 °C for 4 h. the resultant was concentrated by evaporation, dissolved in $CHCl_3$ (50 mL) and washed with an aqueous NaOH solution (0.1 M, 3 x 30 mL). The organic layer collected was dried with anhydrous Na_2SO_4 and the solvent was removed under vacuum. The semisolid residue was dissolved in EtOH (50 mL) and precipitated by addition of an aqueous HCl (37%) solution as its HCl salt, which was washed with EtOH and $CHCl_3$, and dried under vacuum (0.95 g, yield 73%). Anal. calcd. for $C_{34}H_{36}N_3Cl_3 \cdot 5H_2O$: C 59.78, H 6.79, N 6.15. Found: C 59.38, H 5.32, N 5.69. ^{1}H NMR (DMSO, 400 MHz): δ(ppm) 8.80 (s, 2H, H10), 8.60 (d, 4H, H1,8, $J_{1,2}$ 9 Hz), 8.18 (d, 4H, H4,5, $J_{3,4}$ 8 Hz), 7.67 (t, 4H, H2,7, $J_{2,3}$ 7 Hz), 7.61 (t, 4H, H3,6), 5.32 (s, 4H, $H1_{AL}$), 3.81-3.72 (m, 4H, $H2_{AL}$, $J_{2AL,3AL}$ 6 Hz), 3.55-3.47 (m, 4H, $H3_{AL}$). ^{13}C NMR (DMSO, 400 MHz): δ(ppm) 130.83, 130.65, 129.90, 128.98, 127.04, 125.50, 124.55, 122.76, 43.64, 42.81, 42.76. ESI MS (m/z) 484.2752 (z = 1, [**L1** + H]$^+$).

N1,N3-bis(9-anthrylmethyl)dipropylenetriamine (L2). This product was obtained from 9-anthraldehyde (0.32 g, 1.52 mmol) and dipropylenetriamine (0.1 g, 0.76 mmol) in a mixture solvent of EtOH/CH_3CN 50:50 v/v (100 mL) by using the same procedure reported for **L1**. (0.32 g, yield 65%). Anal. calcd. for $C_{36}H_{39}N_3Cl_2 \cdot H_2O$: C 71.75, H 6.86, N 6.97. Found: C 71.09, H 7.28, N 7.36. ^{1}H NMR (DMSO, 10% D_2O, 400 MHz): δ(ppm) 8.72 (s, 2H, H10), 8.34-8.25 (m, 4H, H1,8), 8.17-8.10 (m, 4H, H4,5), 7.71-7.63 (m, 4H, H2,7), 7.60-7.53 (m, 4H, H3,6), 5.17 (s, 4H, $H1_{AL}$), 3.78-3.27 (m, 4H, $H2_{AL}$ $J_{2AL,3AL}$ 6 Hz), 3.09-2.97 (m, 4H, $H4_{AL}$ $J_{3AL,4AL}$ = 7 Hz), 2.16-2.03 (m, 4H, $H3_{AL}$). ^{13}C NMR (DMSO, 10% D_2O, 400 MHz): δ(ppm) 131.84, 131.39, 131.28, 130.31, 128.80, 166.77, 124.27, 122.57, 45.90, 45.21, 43.73, 23.24. ESI MS (m/z) 512.3076 (z = 1, [**L2** + H]$^+$); 256.2635 (z = 2, [**L2** + 2H]$^{2+}$).

ESI-mass spectrometry

Stock solutions 10^{-3} M of the compounds were prepared dissolving the samples in MeOH. The ESI mass study was performed using a TripleTOF® 5600+ high-resolution mass spectrometer (Sciex, Framingham, MA, USA), equipped with a DuoSpray® interface operating with an ESI probe. Respective ESI mass spectra were acquired through direct infusion at 7 μL min^{-1} flow rate. For the determination of the **L1**·KP_n and **L2**·KP_n (where n = 1 or 2) adducts, 10 μM solution of **L1** and **L2** with two equivalents of ketoprofen in MeOH were prepared. The ESI mass study was performed

using a Waters Xevo G2-XS QTof mass spectrometer. ESI mass spectra were acquired through direct infusion at 10 μL min^{-1} flow rate.

Electronic absorption and fluorescence measurements

Absorption and fluorescence spectra were recorded on a Thermo Scientific Evolution 220 spectrophotometer and on a Jasco FP-750 spectrofluorimeter, respectively. An excitation wavelength of 340 nm was used to record fluorescence spectra of ligands. All measurements were performed at 298.0 ± 0.1 K, with ligand concentrations 1 x 10^{-5} M.

Potentiometric measurements

Potentiometric (pH-metric) titrations, employed to determine ligand protonation and metal complexation constants, were performed in H_2O/EtOH 50:50 v/v, with 0.1 M NMe_4Cl as ionic strength, at 298.1 ± 0.1 K using an automated apparatus and a procedure previously described.[1] A small addition of DMSO (1 ml every 30 ml of H_2O/EtOH solution) was required to improve ligand solubility. Acquisition of the emf data was performed with the computer program PASAT.[2,3] The combined Metrohm 6.0262.100 electrode was calibrated as an hydrogen-ion concentration probe by titration of previously standardized amounts of HCl solutions with CO_2-free NMe_4OH solutions and determining the equivalent point by Gran's method,[4] which gives the standard potential, E°, and the ionic product of water (experimental pK_w = 14.58(1) in above stated conditions). The computer program HYPERQUAD[5] was used to calculate the protonation constants of the receptors and substrates and the stability constants of the adducts from the potentiometric data. The concentration of ligands was about 5 × 10^{-4} M in all experiments while the concentrations of ketoprofen were in the range 0.5 × 10^{-4}–5 × 10^{-3} M. The studied pH range was 2.5–8.5 for L1 and 2.5-7.5 for L2. Precipitation of fully deprotonated **L1** and **L2** is observed at pH > 9.0.

Description of the protonation features of L1 and L2.

Considering the values of the protonation constants of the receptors (see Table S1), the basicity of diethylenetriamine (dien) steadily drops when benzyl- or napththyl fragments are appended on its terminal amine groups, e.g., moving from dien to its terminal benzyl (log K_1 = 9.4) and naphthyl (logK_1 = 8.38) terminal bis-derivatives (see reference 20). Data for our anthracenyl derivatives (here **L1** comparison is fully relevant, with the caveat of our study being in a mixed solvent) appear in keeping with these reports. Therefore, log K of about 7.8 log units for L1 is in line with previous data.

What is different with our ligands, in comparison to naphthyl derivatives, is that the anthracene residue decreases terminal amino group basicity to the point where the central amino group becomes the most basic, *i.e.*, the one subject to the first protonation equilibrium, while in naphthyl derivatives protonation of terminal amino groups is observed first. This can be due to higher hydrophobic character of anthracene, which does not favour protonation of an adjacent amine group and consequent formation of a highly hydrated ammonium group. In the naphthyl derivative, entrance of a second proton implies proton migration to the two terminal amino groups and turns on fluorescence. The detection of KP in our case happens on a similar proton transfer basis.

The protonation constants of the bis-naphthyl derivative are log K_1 = 8.38, log K_2 = 7.81 log K_3 = 3.81, which are in line with the **L1** values, according for the reduced basicity brought about by the anthracene residue.

The situation appears to be somewhat different for **L2**. **L2** is found less basic than **L1** in the first protonation, happening again on the central amino group. This lowering of basicity is attributed to the increased N-N distance (propylenic spacer) and the impossibility for the lateral amino groups in participating in proton binding (which is attested instead for ethylenediamine, ref. 20).

Second protonation has an almost identical log K with respect to **L1**, as the two lateral amino groups are protonated for both ligands and the repulsion among them in aqueous environment is minimal with both 5 or 7 bonds in-between (see reference 20a of the manuscript).

Lack of third protonation for **L2** or, better, its happening at acidic pH falling outside measurement range, must have a more subtle nature. Successive protonation steps of polyamines tend to be less and less exothermic while, in general, they tend to remain entropically favourable at all stages. The favourable entropic contribution arises from the partial charge-neutralization process tied to H^+ binding, which results in significant desolvation effects (solvent molecules return to the bulk, thus gaining degrees of freedom). Since (i) **L1** is already poorly basic in its third protonation step, (ii) it is inherently less flexible than **L2**, and (iii) **L1** must already be somewhat stiffer than **L2** when both ligands are in diprotonated form (somewhat more electrostatic repulsion), the reduced basicity of **L2** in the third protonation step might arise from its superior flexibility and to the increased loss of conformational degrees of freedom associated with the third protonation step.

NMR measurements

NMR titrations were carried out by using a Bruker Avance 400 MHz instrument, in D_2O/CD_3OD 30:70 (vol/vol) mixture at pH 7, by addition of KP to 0.01 M solutions of **L1** or **L2** or by addition of **L1** or **L2** to a 0.01 M solution of KP. The pH was adjusted at 7 by adding small amounts of NaOD or DCl after each addition of the receptors to solutions of KP or of KP to solutions of **L1** or **L2**.

Limit of Detection (LOD) determination

The detection limit was determined from the fluorescence titrations data based on a reported method.[6] The fluorescence spectrum of the probes (**L1**, **L2** and $[Zn\mathbf{L2}]^{2+}$) at pH 7 in H_2O/EtOH 50:50 (Vol/Vol) was measured by six times and the standard deviation of blank measurement was achieved. To gain the slop, the fluorescence intensity data at 414 nm was plotted as a concentration of KP. So, the detection limit was calculated with the following equation:

Detection limit (LOD)=$3\sigma/S$

where σ is the standard deviation of blank measurement and S is the slope between the fluorescence versus KP concentration.

X-ray crystallographic experimental details.

Crystals of compound $(H_2\mathbf{L2})_2 \cdot \mathbf{0.75EtOH} \cdot \mathbf{2.75H_2O}$ **(1)** were obtained by slow evaporation of a solution of **L2** and KP (2 equivs.) in H_2O/EtOH 50:50 (vol/vol) at neutral pH.
Intensity data for compound **1** were collected at 100 K by using a Bruker Apex-II CCD diffractometer. Data were collected with the Bruker APEX2 program[7] and integrated and reduced with the Bruker SAINT software,[8] absorption correction was performed with SADABS-2016/2.[9] Radiation used was Cu−Kα (λ = 1.54184 Å).
The crystal structure was solved using the SIR-2004 package[10] and refined by full-matrix least squares against F^2 using all data (SHELXL-2018/3).[11] All non-hydrogen atoms, except for those of the solvent molecules, were refined with anisotropic displacement parameters. The hydrogen

atoms bonded to the nitrogen atoms of the **L2** ligand were found in the Fourier difference map and their coordinated were freely refined while their thermal parameters were set in accordance to the one of the atoms to which they are bonded. All the other hydrogen atoms of the ligand and of the ketoprofen anions were set in calculated position. The ethanol molecules and all the 2.75 water molecules present in the asymmetric unit were in disordered position. Such disorder was modelled using for the ethanol molecule two position (occupancy factors were set to 0.5 and 0.25 for the two models), and for the water molecules using three possible positions with occupancy factors ranging from 0.25 and 0.5. Solvent molecules hydrogen atoms were not introduced in the refinement.
Geometrical calculations were performed by PARST97[12] and molecular plots were produced by the program Mercury (v4.3.1)[13] and Discovery Studio Visualizer 2019.[14]
Crystallographic data and refinement parameters are reported in Table S3.

Details of the crystal structure of the $(H_2L2)_2 \cdot 0.75EtOH \cdot 2.75H_2O$ (1)

In the asymmetric unit of **1** (Figure 3), one $H_2\mathbf{L2}^{2+}$ cation, two KP anions, 0.75 ethanol molecules and 2.75 water molecules are present. All the solvent molecules are in disordered position.
The $H_2\mathbf{L2}^{2+}$ cation takes an open arrangement with the chain connecting the two anthracene moieties showing an all-trans conformation (see Table S4, Figure 3) and the two anthracene rings forming each other an angle of about 60 degrees.
Concerning the KP anions, in Table S4 the dihedral angles τ1, τ2, τ3 (see Scheme S2) and the angle between the two aromatic rings for the six structures are reported. On the basis of these torsion angles, the conformation of the two KP anions can be described as (+ac)(+ac)(sp) and (+ac)(sp)(-sc) for the S and R enantiomer, respectively. These conformations were compared with those of seven compounds[15-19] containing ketoprofen retrieved in the Cambridge Structural Database (CSD, v 5.41)[20]; interestingly none of them show a value for τ2 comparable with that observed in the S enantiomer (see Figure 3 and Tables S4 and S5).
Concerning the crystal packing of compound **1**, in Table S6 the H-bonds involving $\mathbf{H_2L2^{2+}}$ cations and ketoprofen anions are reported. Each $H_2\mathbf{L2}^{2+}$ cation is connected, due to the two protonated nitrogen atoms, to four different ketoprofen anion, 2 R and 2 S. In addition, the unprotonated nitrogen atom, N1, interact with the carbonyl oxygen atom of one ketoprofen anion (see Figure S18).
Carbonylic oxygen atom O1B connects two $H_2\mathbf{L2}^{2+}$ cations, the same cations are linked by the C10A(O1AO2A) carbonylic group, as a consequence a $[(H_2\mathbf{L2})_2/4KP]$ unit is formed (see Figure S18). A global perspective of crystal packing features is presented in Figure S19.

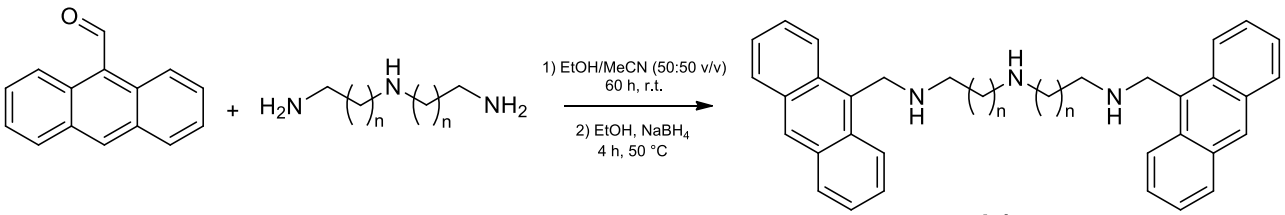

Scheme S1. Synthetic route to obtain ligands **L1** and **L2**

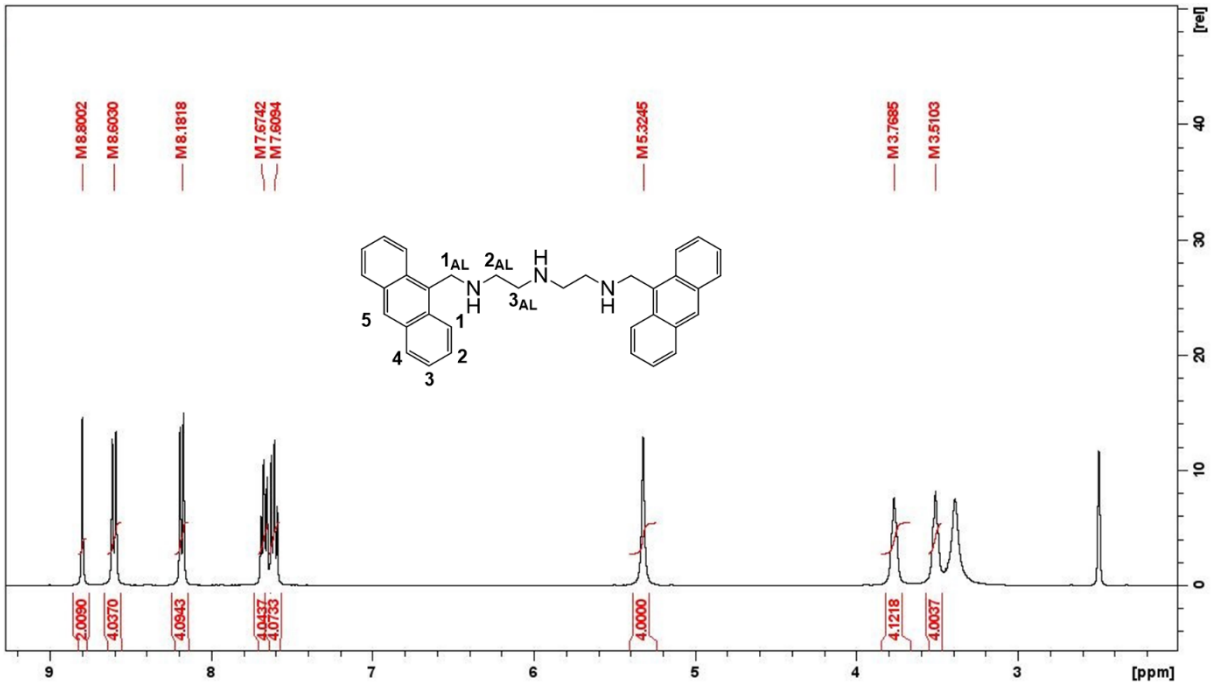

Figure S1. ^{1}H NMR spectrum of compound **L1** (DMSO, 400 MHz, 298 K): δ(ppm) 8.80 (s, 2H, H5), 8.60 (d, $J_{1,2}$=9 Hz, 4H, H1), 8.18 (d, $J_{3,4}$=8 Hz, 4H, H4), 7.67 (t, $J_{2,3}$=7 Hz, 4H, H2), 7.61 (t, 4H, H3), 5.32 (s, 4H, $H1_{AL}$), 3.81-3.72 (m, 4H, $H2_{AL}$), 3.55-3.47 (m, 4H, $H3_{AL}$). The aliphatic signals are affected by line broadening, preventing the estimation of the proton coupling constants.

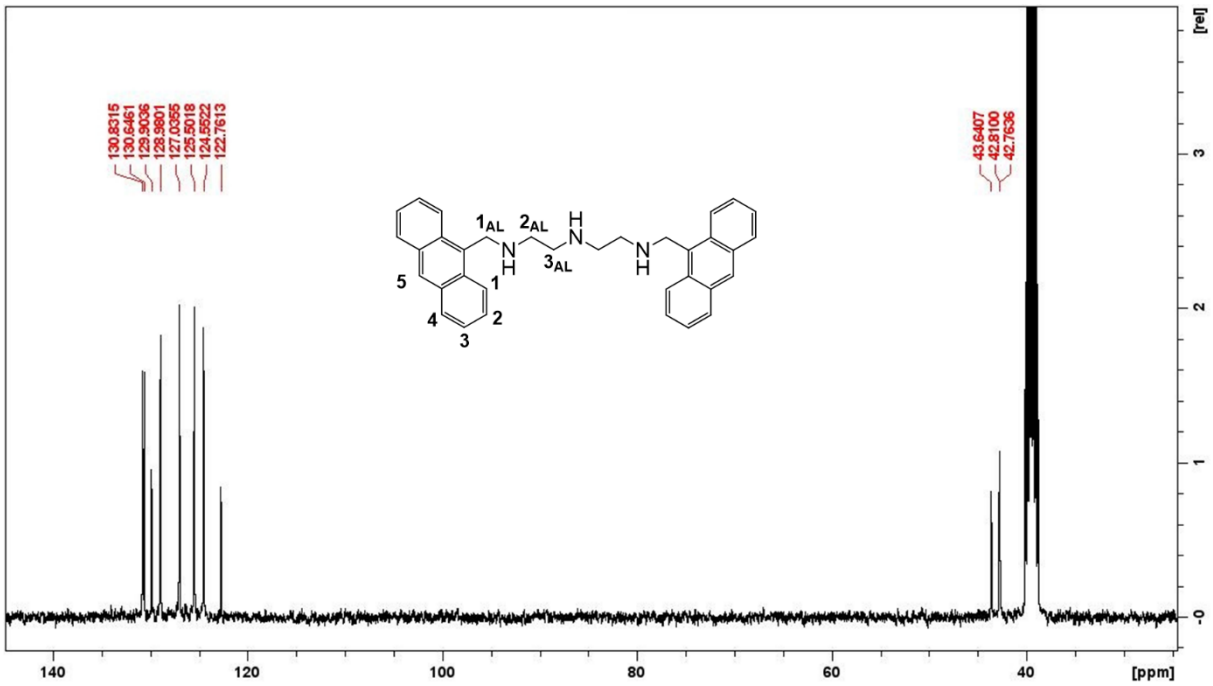

Figure S2. ^{13}C NMR spectrum of compound **L1** (DMSO, 100 MHz, 298 K): δ(ppm) 130.83, 130.65, 129.90, 128.98, 127.04, 125.50, 124.55, 122.76, 43.64, 42.81, 42.76.

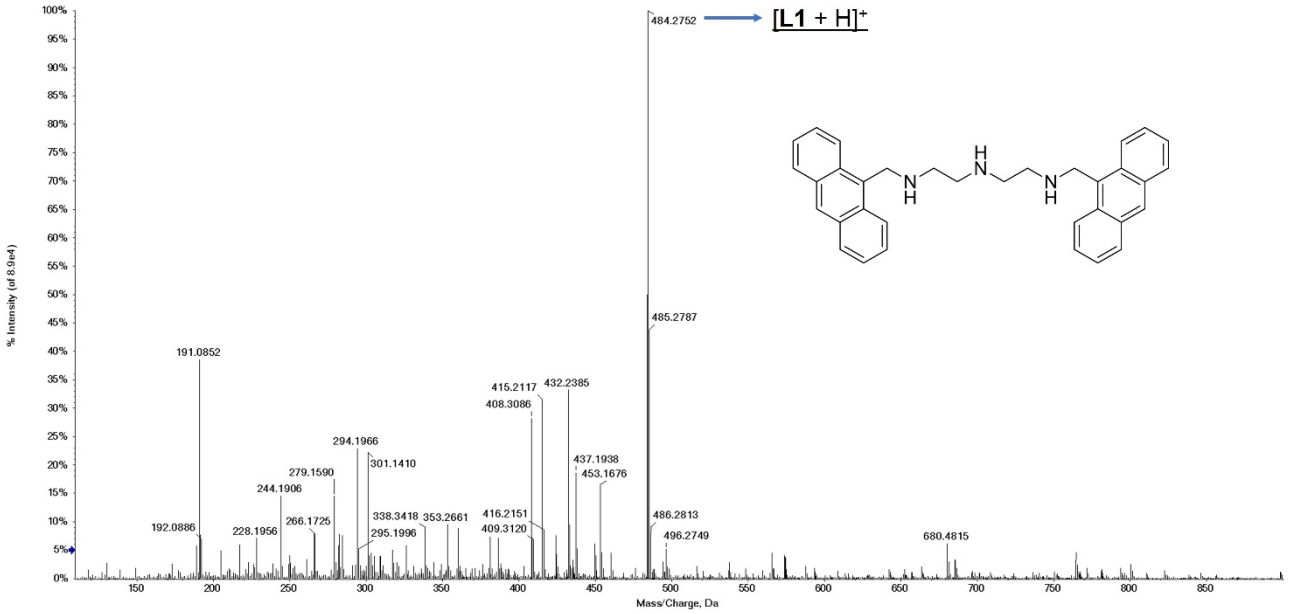

Figure S3. High resolution mass spectrum of compound **L1** in MeOH; 484.2752 (z = 1, [**L1** + H]$^+$).

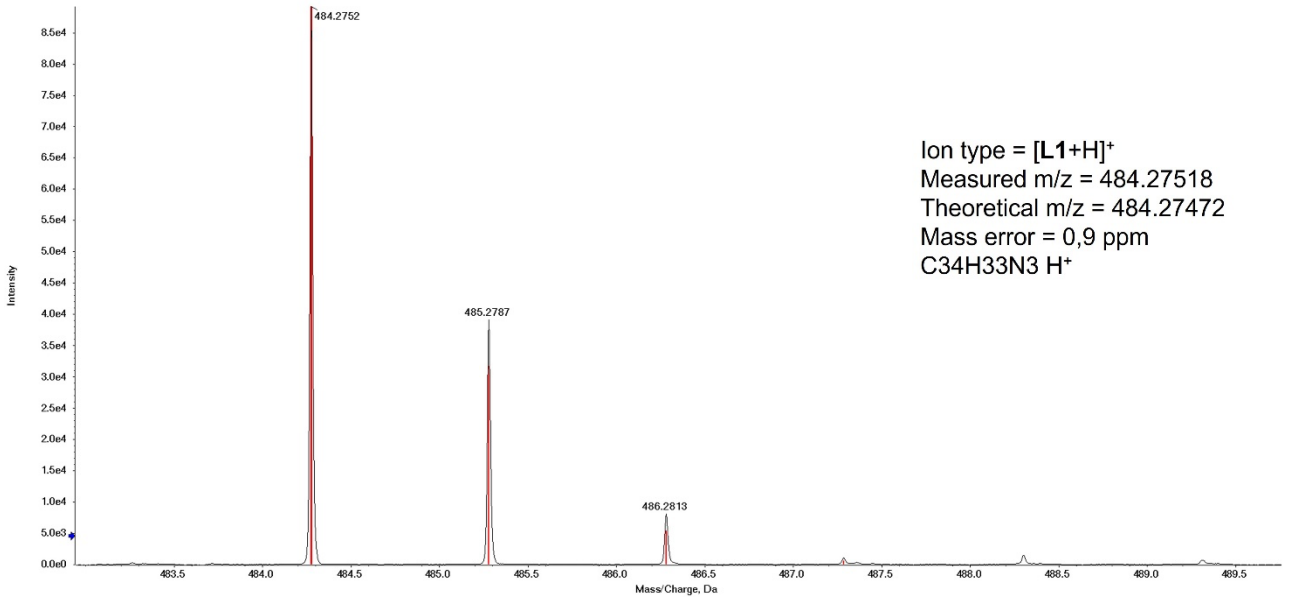

Figure S4. Isotopic pattern of the [**L1**+H]$^+$ (z = 1) ion, with measured (black) and theoretical (red) m/z value of the most abundant isotopic peak, 283.0-490.0 Da region.

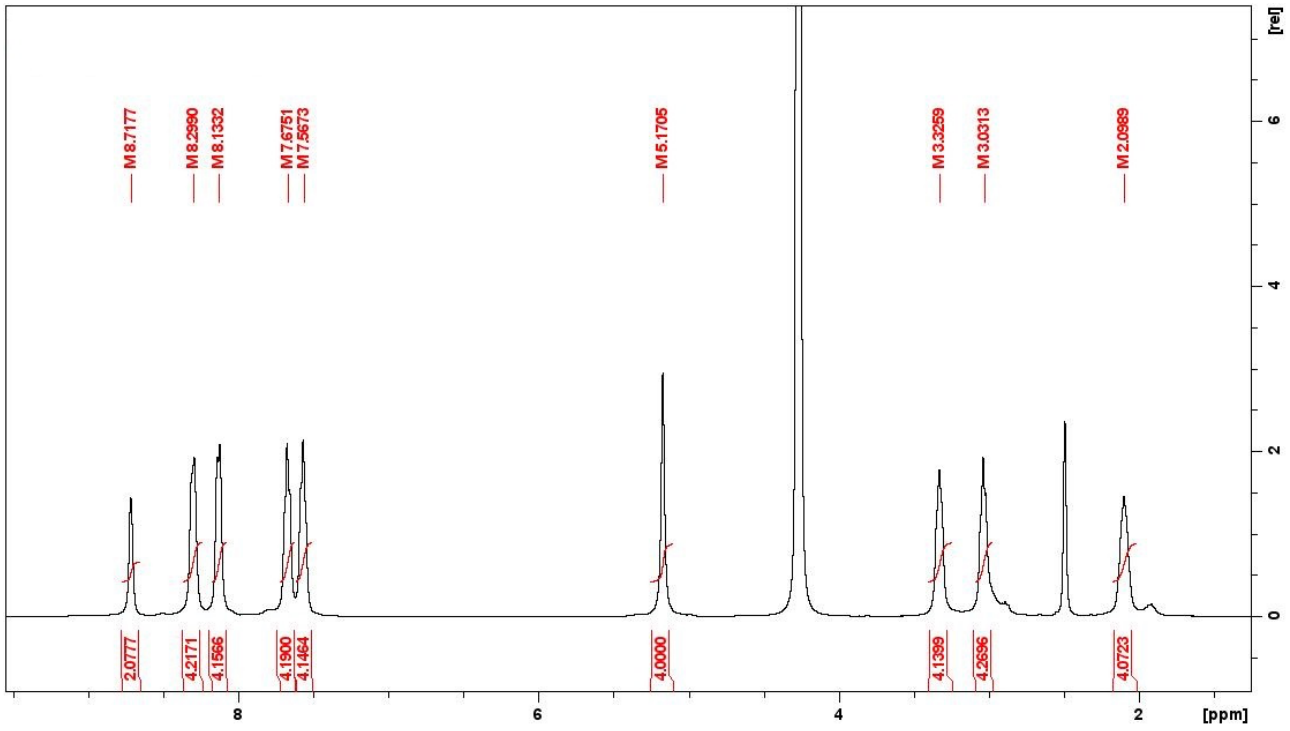

Figure S5. ^{1}H NMR spectrum of compound **L2** (DMSO, 10% D_2O, 400 MHz, 298 K): δ(ppm) 8.72 (s, 2H, H5), 8.34-8.25 (m, 4H, H1), 8.17-8.10 (m, 4H, H4), 7.71-7.63 (m, 4H, H2), 7.60-7.53 (m, 4H, H3), 5.17 (s, 4H, $H1_{AL}$), 3.78-3.27 (m, 4H, $H2_{AL}$), 3.09-2.97 (m, 4H, $H4_{AL}$), 2.16-2.03 (m, 4H, $H3_{AL}$). The spectrum is affected by line broadening, preventing the estimation of the proton coupling constants.

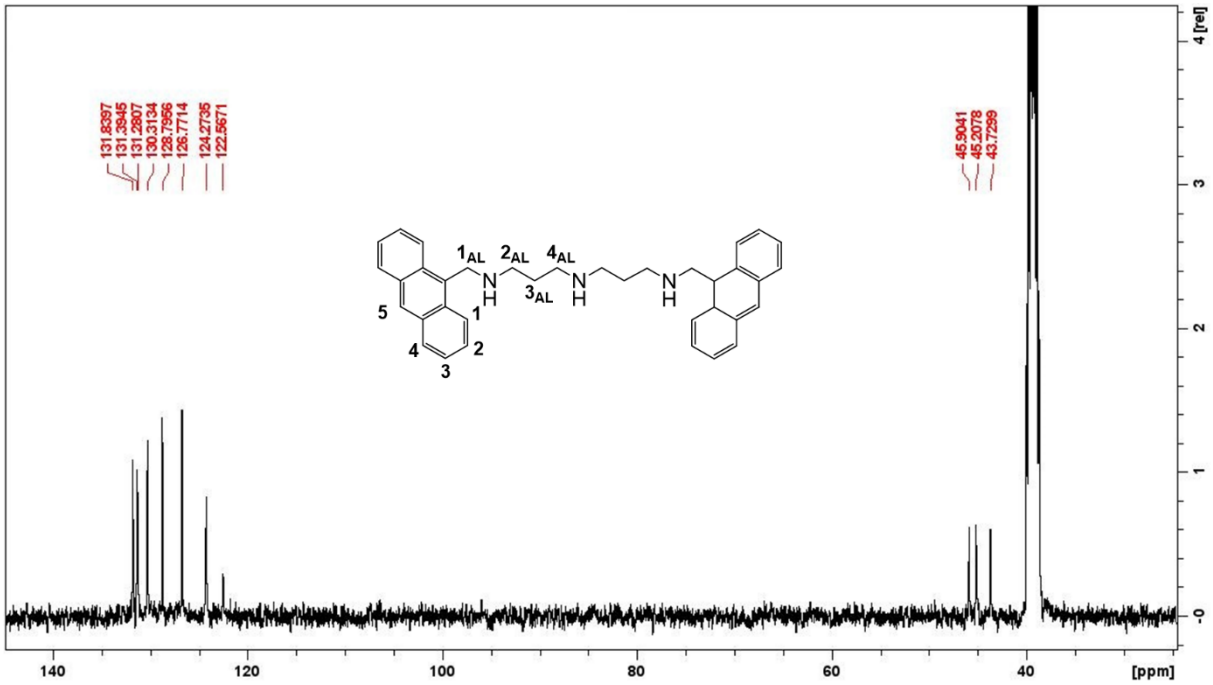

Figure S6. ^{13}C NMR spectrum of compound **L2** (DMSO, 10% D_2O, 100 MHz, 298 K): δ(ppm) 131.84, 131.39, 131.28, 130.31, 128.80, 166.77, 124.27, 122.57, 45.90, 45.21, 43.73, 23.24.

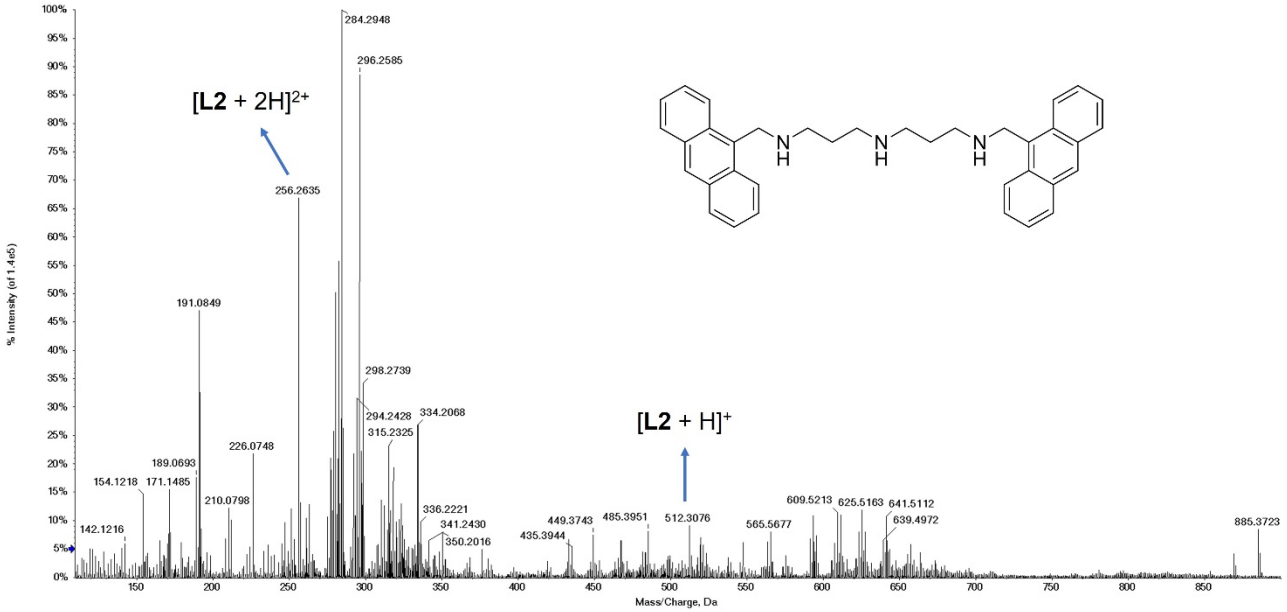

Figure S7. High resolution mass spectrum of compound **L2** in MeOH (0.1% FoA); 512.3076 (z = 1, [**L2** + H]$^{+}$); 256.2635 (z = 2, [**L2** + 2H]$^{2+}$).

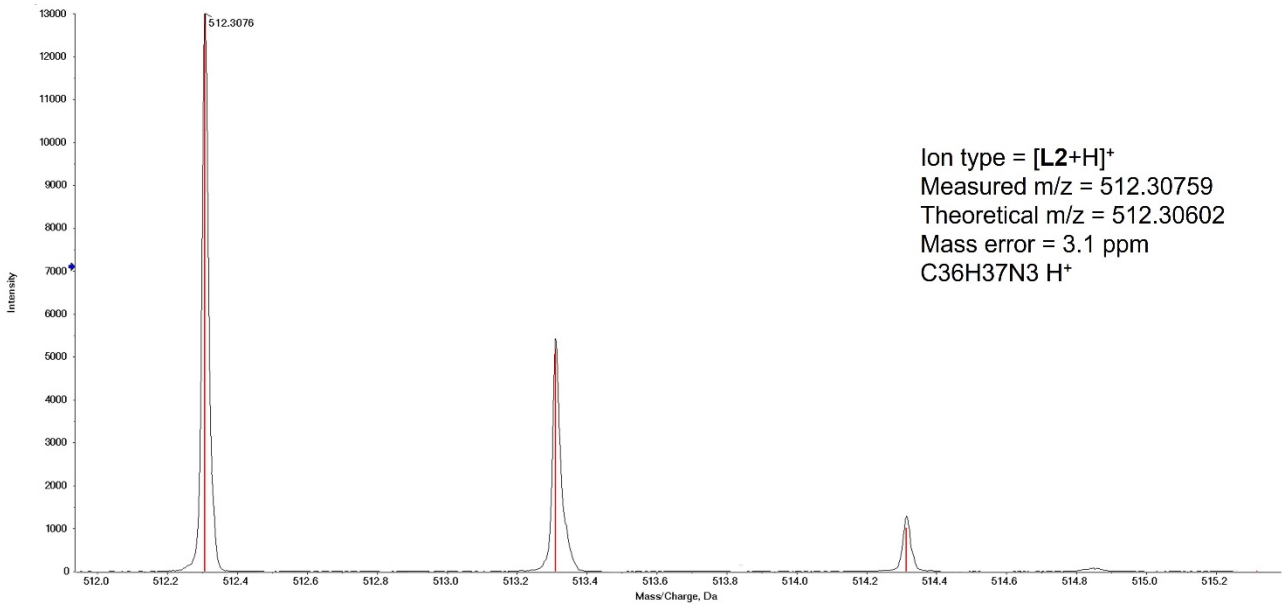

Figure S8. Isotopic pattern of the [**L2** + H]$^{+}$ (z = 1) ion, with measured (black) and theoretical (red) m/z value of the most abundant isotopic peak, 512.1-515.4 Da region.

Equilibrium	L1	L2
$L + H^+ = HL^+$	7.78(5)	6.76(8)
$HL^+ + H^+ = H_2L^{2+}$	5.80(4)	5.84(7)
$H_2L^{2+} + H^+ = H_3L^{3+}$	3.31(7)	-

Table S1. Protonation constants of L1 and L2 at 298.1±0.1 K, 0.1 M NMe_4Cl H_2O/EtOH 50:50 v/v).

	Ketoprofen	Acetate	Benzoate	Ibuprofen
log *K*	5.31(1)	5.41(4)	5.23(2)	5.31(3)

Table S2. Protonation constants of ketoprofen, acetate, benzoate and ibuprofen (298.1±0.1 K, 0.1 M NMe_4Cl H_2O/EtOH 50:50 v/v).

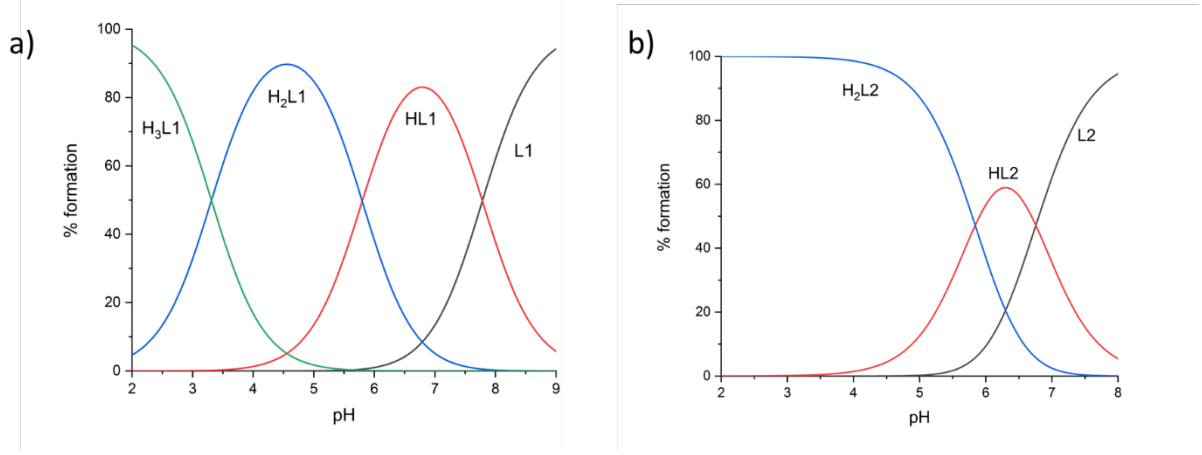

Figure S9. Distribution diagrams of the protonated species of **L1** (a) and **L2** (b) ([**L1**] = [**L2**] = 5×10^{-4} M), calculated on the basis of the equilibrium constants in Table 1 (298.1±0.1 K, 0.1 M NMe_4Cl H_2O/EtOH 50:50 v/v).

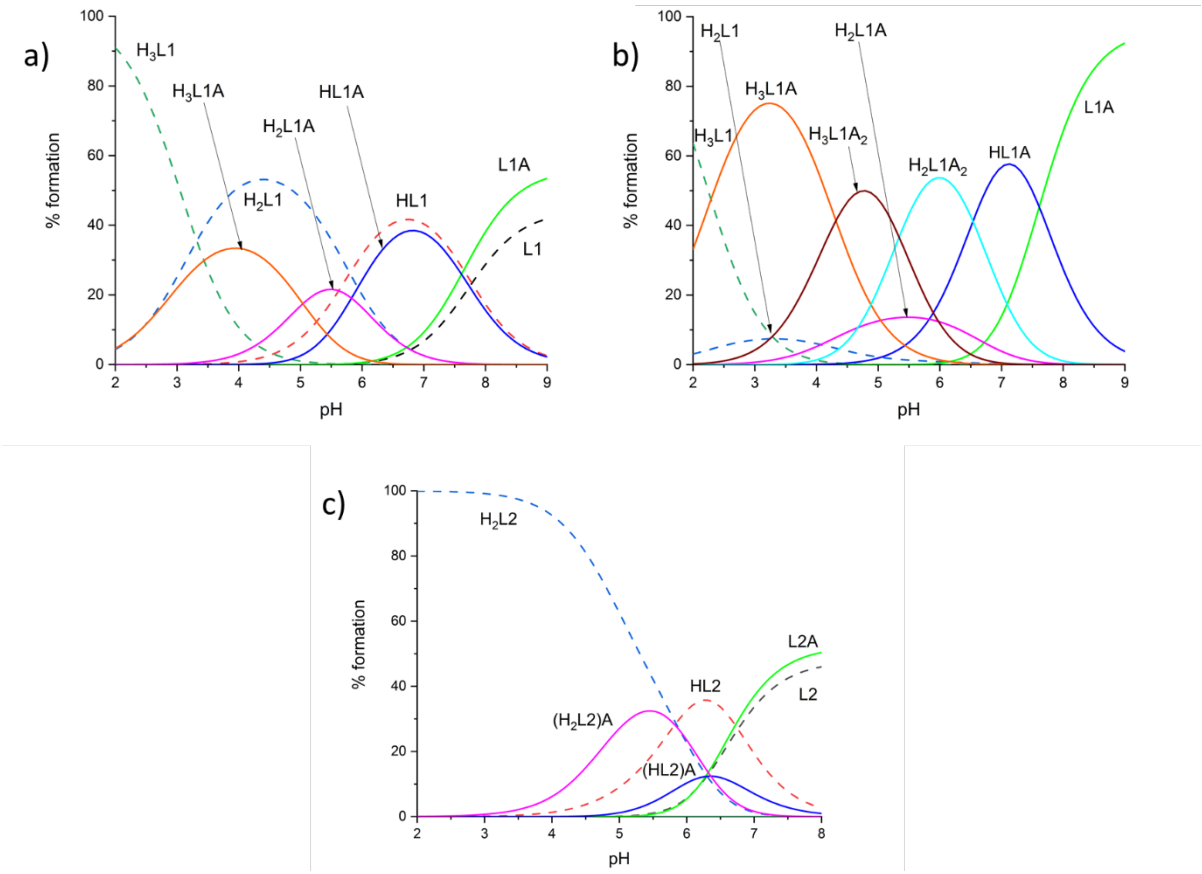

Figure S10. Distribution diagrams of the 1:1 **L1**-ketoprofen (the anionic form of ketoprofen is indicated with A) complexes (a, [**L1**] = [A] = 5×10^{-4} M), 1:2 L1-A complexes (b, [**L1**] = 5×10^{-4} M, [A] = 5×10^{-3} M) and 1:1 **L2**-ketoprofen complexes (b, [**L2**] = 5×10^{-4} M, [A] = 1.5×10^{-3} M) calculated on the basis of the equilibrium constants in Table 1. Dashed lines refer to uncomplexed ligand species ((298.1±0.1 K, 0.1 M NMe_4Cl H_2O/EtOH 50:50 v/v).

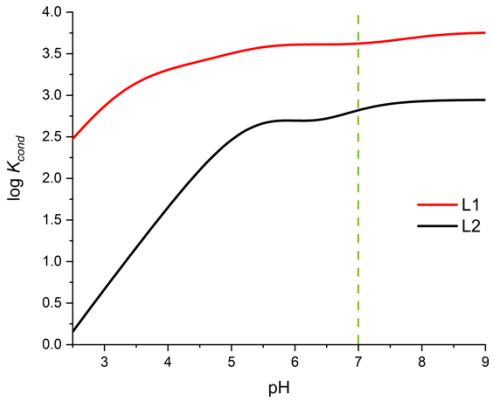

Figure S11. pH dependence of the conditional constants for **L1** and **L2**. K_{cond} = Σ[Hi+jLA]/(Σ[HiL] × Σ[HjA]), with **L**=**L1** or **L2**, i and j number of acidic protons on the ligand and on the anion, respectively (298.1±0.1 K, 0.1 M NMe_4Cl H_2O/EtOH 50:50 v/v).

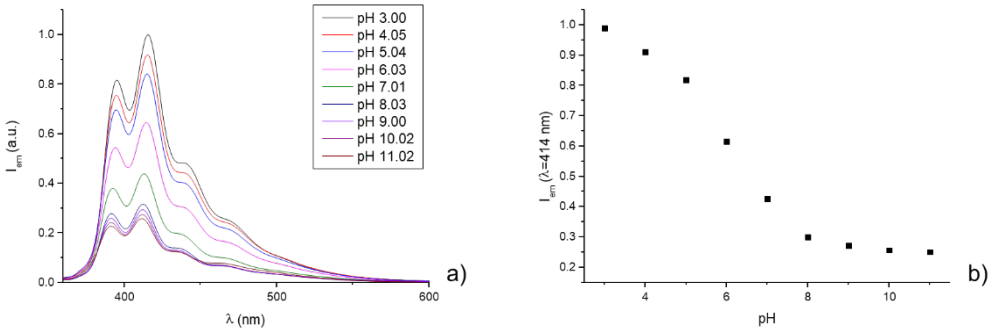

Figure S12. (a) Fluorescence spectra of **L1** at different pH values in H_2O/EtOH 50:50 (Vol/Vol) and (b) plot of the fluorescence emission at 414 nm as function of pH ([**L1**] = 10^{-5} M, λ_{exc} = 340 nm, 298 K).

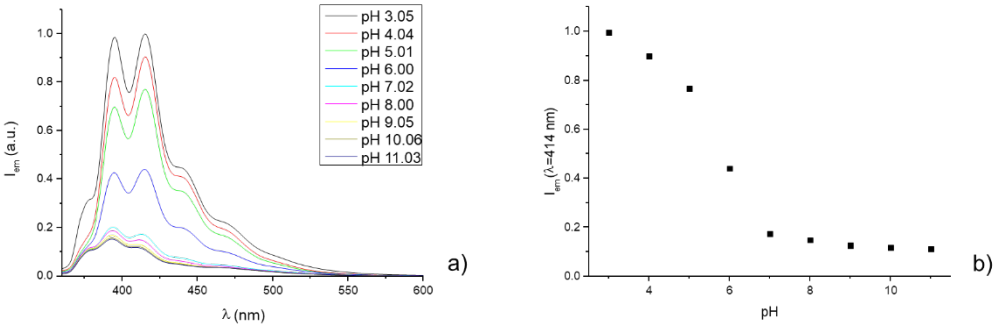

Figure S13. (a) Fluorescence spectra of **L2** at different pH values in H_2O/EtOH 50:50 (Vol/Vol) and (b) plot of the fluorescence emission at 414 nm as function of pH ([**L2**] = 10^{-5} M, λ_{exc} = 340 nm, 298 K).

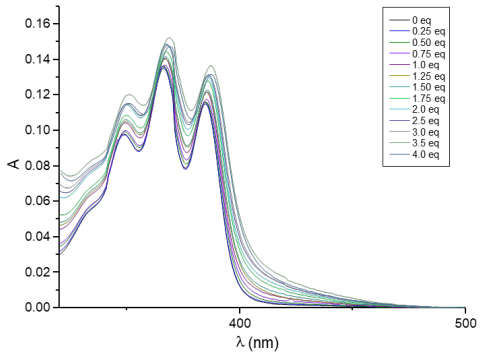

Figure S14. Absorption spectra of **L1** at pH 7 (0.001 M TRIS buffer) in H_2O/EtOH 50:50 (Vol/Vol) in the presence of increasing amounts of ketoprofen ([**L1**] = 10^{-5} M, 298 K).

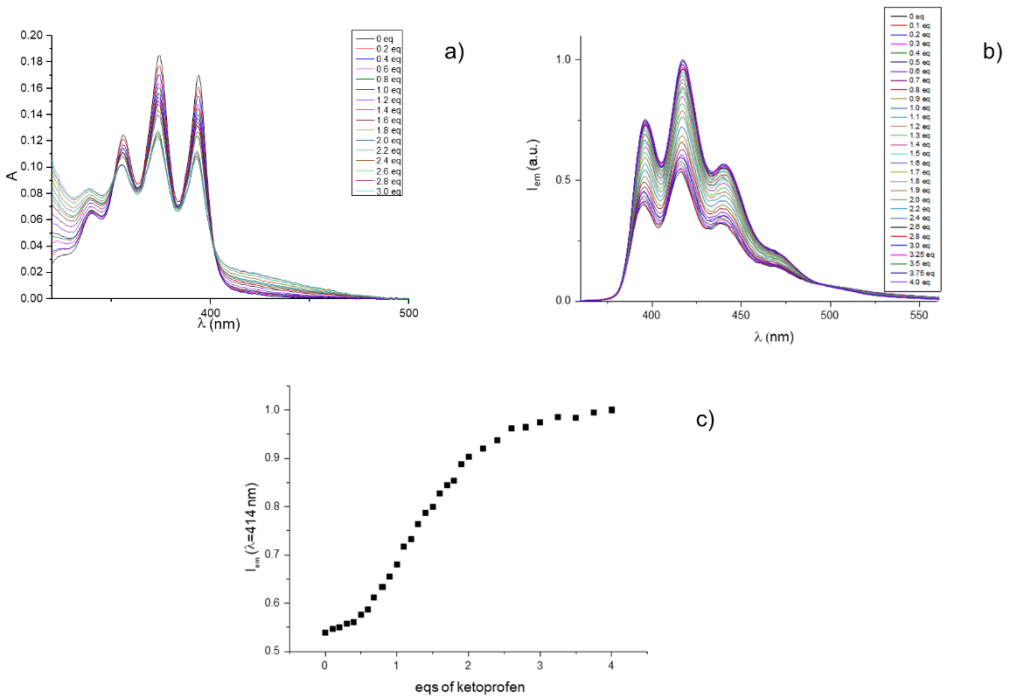

Figure S15. (a) Absorption and (b) emission spectra of **L2** at pH 7 (0.001 M TRIS buffer) in H_2O/EtOH 50:50 (Vol/Vol) in the presence of increasing amounts of ketoprofen ([**L2**] = 10^{-5} M, λ_{exc} = 340 nm, 298 K). (c) Plot of the fluorescence emission of **L2** at 414 nm.

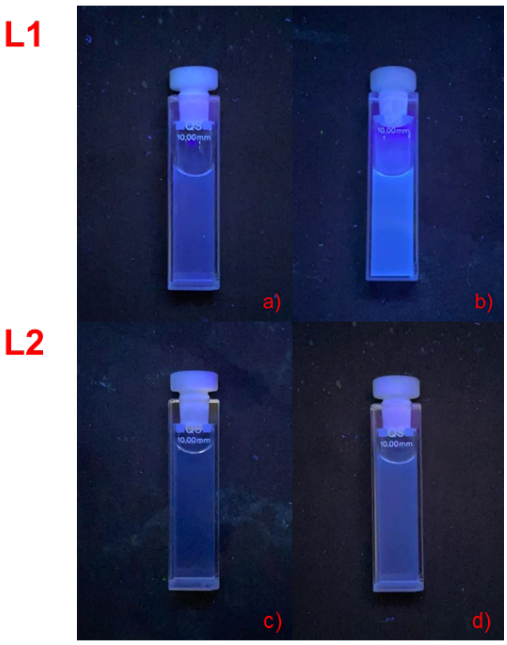

Figure S16. Images of **L1** (a and b) and **L2** (c and d) at pH 7 (0.001 M TRIS buffer) in H_2O/EtOH 50:50 (Vol/Vol), under UV lamp (λ_{exc} = 366 nm, 298 K) before (a and c) and after (b and d) the addition of 10 equivalents of ketoprofen. ([**L1**] = [**L2**] =10^{-5} M).

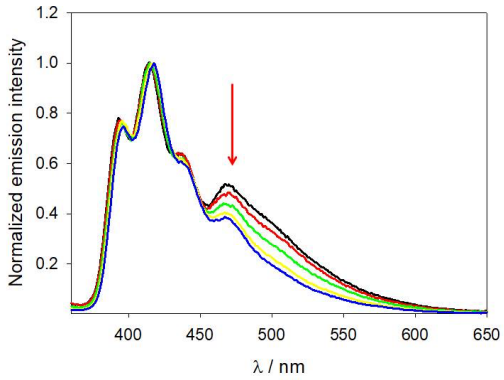

Figure S17. Fluorescence emission spectra of **L1** at pH 7 (0.001 M TRIS buffer) in H_2O/EtOH 50:50 (Vol:Vol) normalized on the maxima in presence of 0 (black), 1 (red), 2 (green), 3 (yellow) and 4(blue) equivalents of ketoprofen ([**L1**] = 10^{-5} M, λ_{exc} = 340 nm, 298 K).

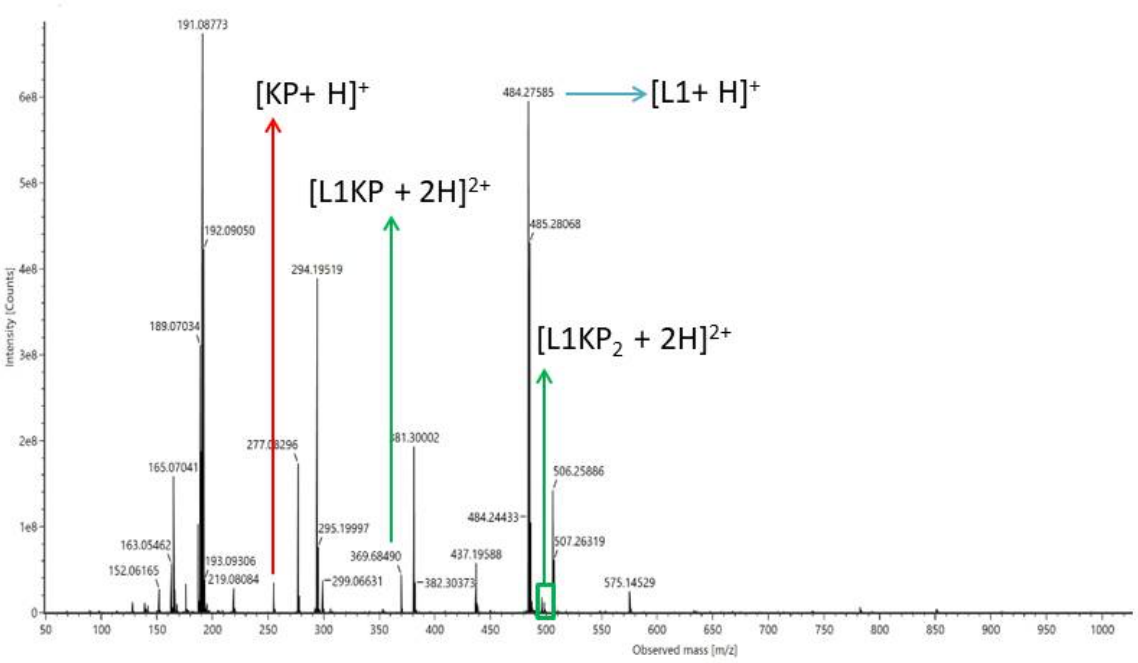

Figure S18. High resolution mass spectrum of in the presence of **KP (2 equivs.)** in MeOH: 255.1012 (z = 1, $[KP + H]^+$), 369.6849 (z = 2, $[\mathbf{L1}(KP) + 2H]^{2+}$), 484.2752 (z = 1, $[\mathbf{L1} + H]^+$), 496.73547 (z = 2, $[\mathbf{L1}(KP)_2 + 2H]^{2+}$).

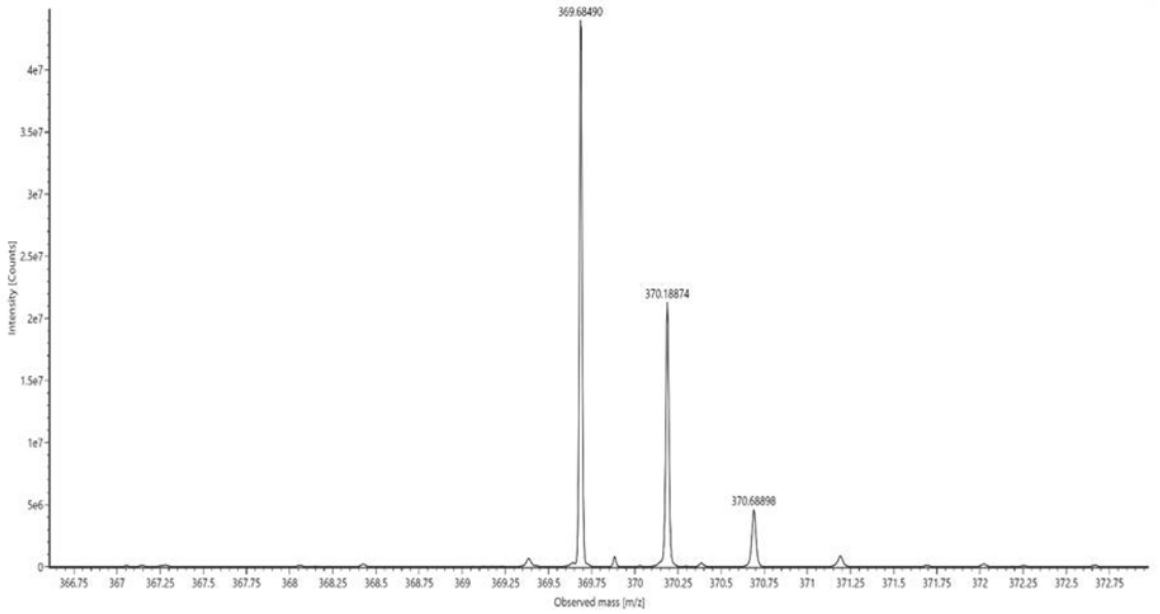

Figure S19. Isotopic pattern of the 1:1 adduct $[\mathbf{L1}(KP)_2 + 2H]^{2+}$ (z = 2) ion, with measured m/z values.

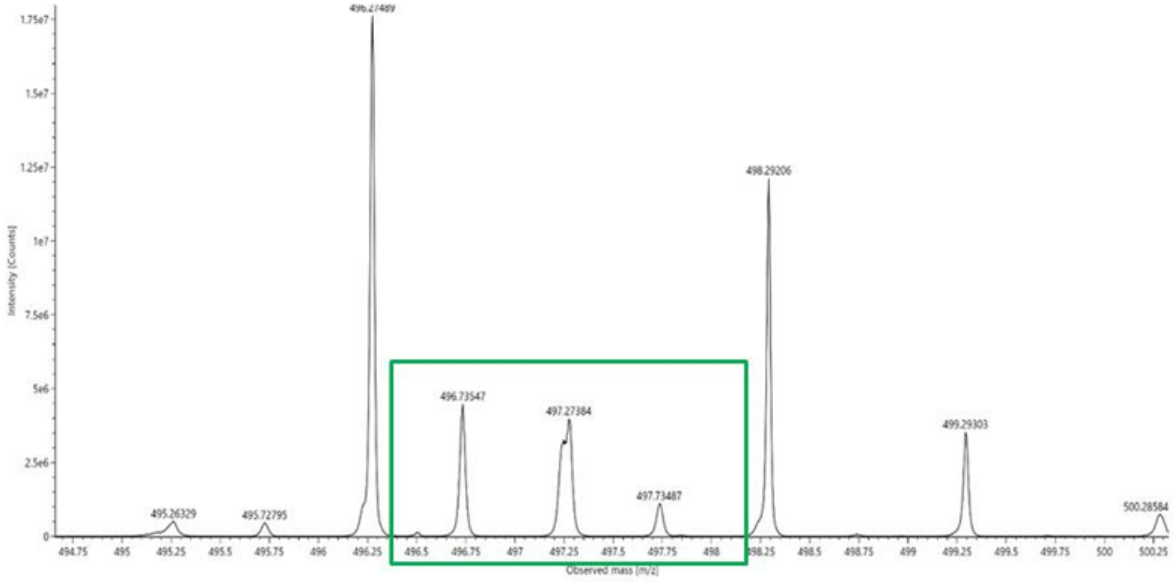

Figure S20. Isotopic pattern of the 1:2 adduct $[\mathbf{L1}(KP)_2 + 2H]^{2+}$ (z = 2) ion, with measured m/z values.

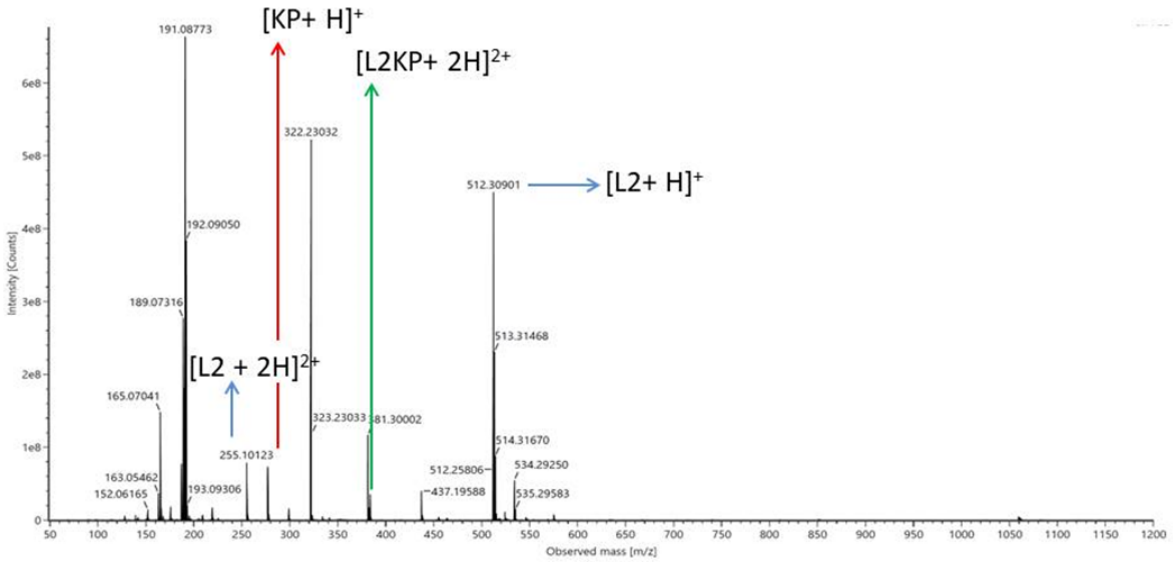

Figure S21. High resolution mass spectrum of **L2** in the presence of KP (2 equivs.) in MeOH: 255.1012 (z = 1, $[KP + H]^+$), 256.2635 (z = 2, $[\mathbf{L2} + 2H]^{2+}$), 383.7015 (z = 2, $[\mathbf{L2}(KP) + 2H]^{2+}$), 510.74916 (z = 2, $[\mathbf{L2}(KP)_2 + 2H]^{2+}$), 512.3090 (z = 1, $[\mathbf{L2} + H]^+$).

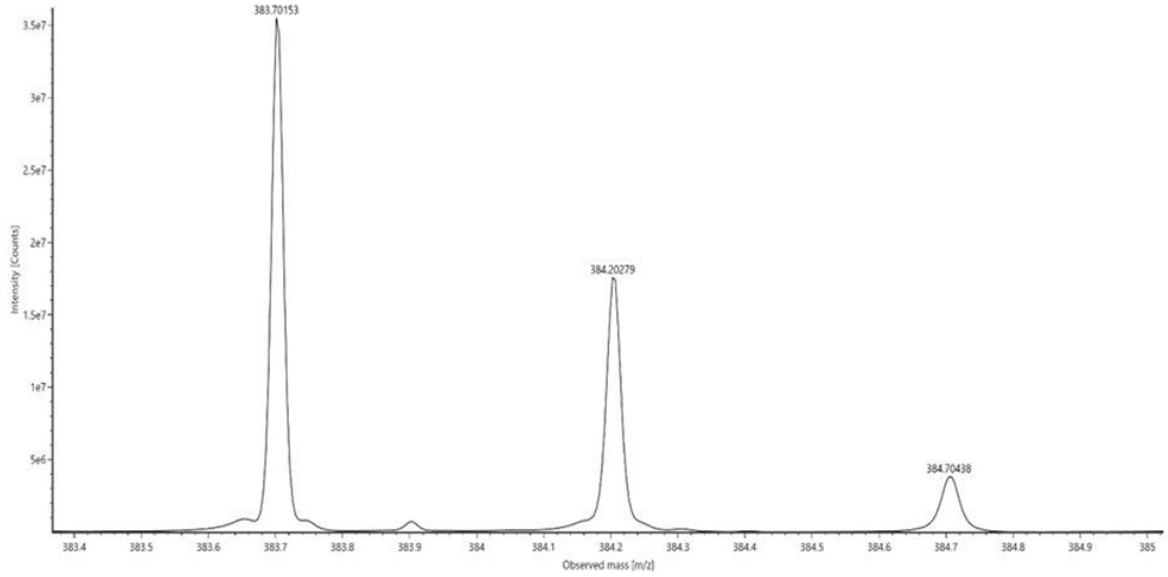

Figure S22. Isotopic pattern of the 1:1 adduct $[\mathbf{L2}(KP) + 2H]^{2+}$), (z = 2) ion, with measured m/z values.

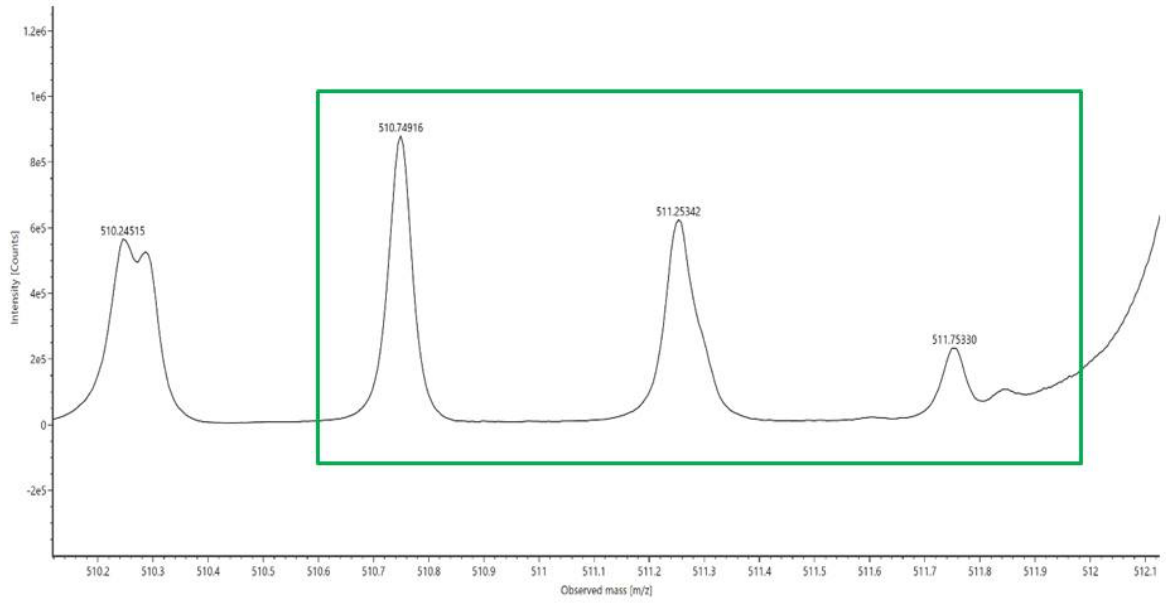

Figure S23. Isotopic pattern of the 1:2 adduct [**L2**$(KP)_2$ + 2H]$^{2+}$), (z = 2) ion, with measured m/z values.

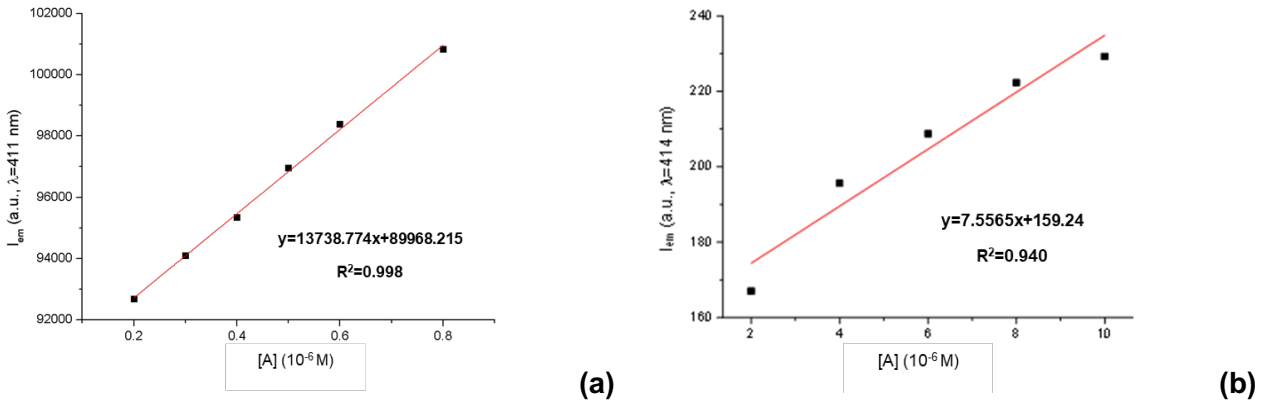

Figure S24. Plot of fluorescence emission of **L1** ([**L1**] =10^{-5} M, λ_{exc}=340 nm, σ=981.375) (a) and **L2** ([**L2**] = 10^{-5} M, λ_{exc} = 340 nm, σ = 0.712) (b) at pH 7 (0.001 M TRIS buffer) in H_2O/EtOH 50:50 (Vol/Vol) in the presence of increasing amount of ketoprofen at 298 K. The detection limit was calculated to be 0.21 μM for **L1** and 0.24 μM for **L2**.

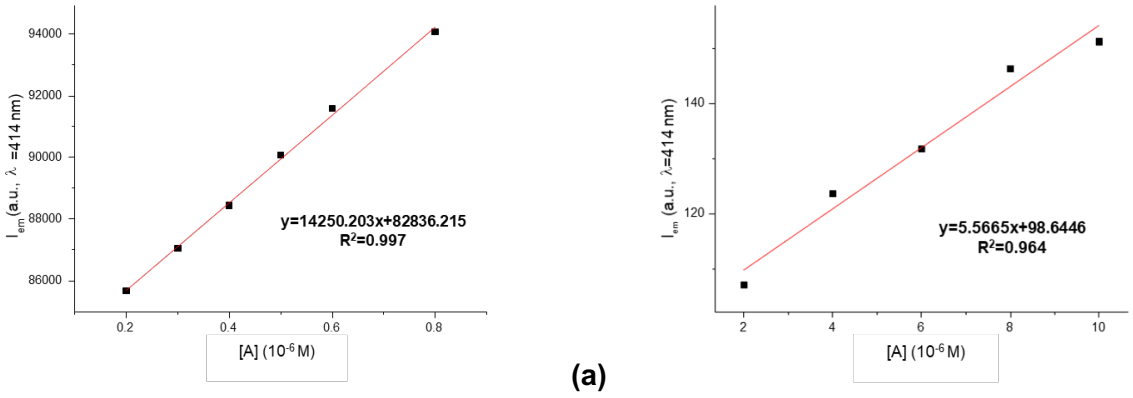

Figure S25. Plot of fluorescence emission of **L1** ([**L1**] = 10^{-5} M, λ_{exc} = 340 nm, σ = 1679.534) and **L2** ([**L2**] = 10^{-5} M, λ_{exc} = 340 nm, σ = 0.7473) at pH 7 in tap water/EtOH 50:50 (Vol/Vol) in the presence of increasing amount of ketoprofen at 298 K. The detection limit was calculated to be 0.35 μM for **L1** and 0.40 μM for **L2**. Tap water characteristics: NH_4^+, 0.05 mg/L; total As, 1 μg/L; Ca^{2+}, 55 mg/L; free Cl residue 0.29 mg/L; Cl^- 48 mg/L; Mg^{2+}, 12 mg/L; total Mn 2 mg/L; NO_3^- 5 mg/L; K^+ 4 mg/L; Na^+ 32 mg/L; SO_4^{2-} 53 mg/L; hardness, 18 °f; fixed residue 365 mg/L; pH 7.2.

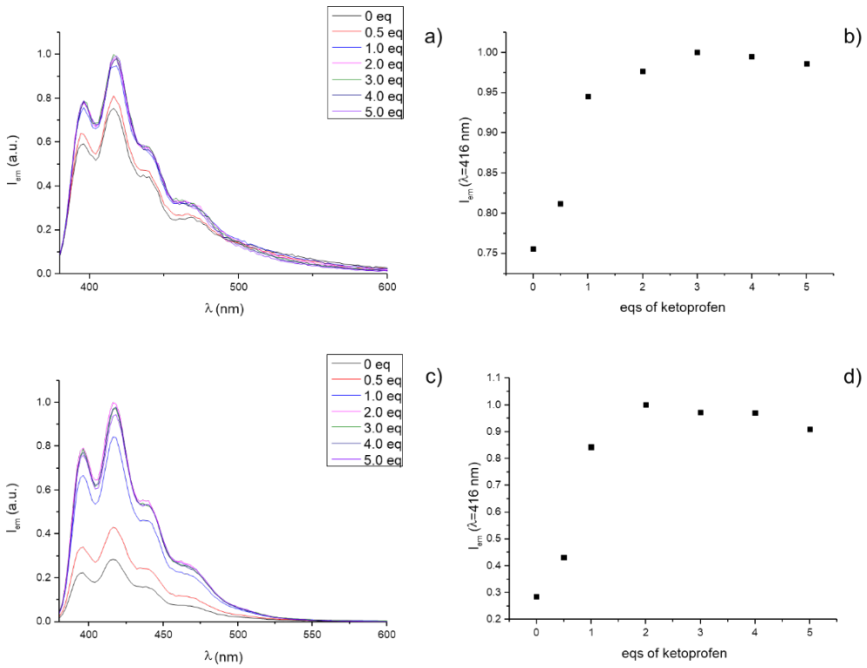

Figure S26. Emission spectra of **L1** (a) and **L2** (c) at pH 7 (0.001 M TRIS buffer) in H_2O in the presence of increasing amounts of ketoprofen at 298 K ([**L1**] = 10^{-5} M, [**L2**] = 10^{-5} M, λ_{exc} = 340 nm) and plots of the fluorescence emission of **L1** (b) and **L2** (d) at 416 nm.

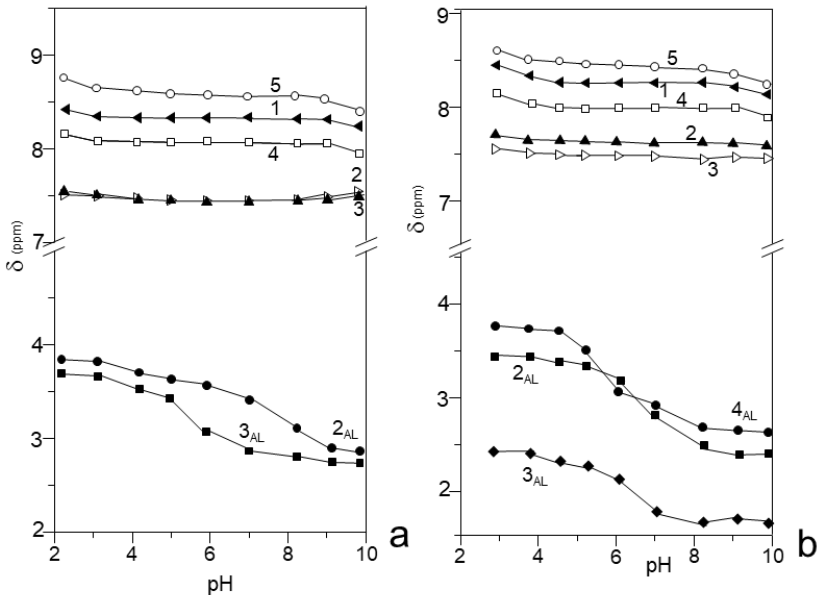

Figure S27. pH dependence of ^{1}H NMR signals of **L1** (a) and **L2** (b) as a function of pH (D_2O/C_2D_5OD 30:70 Vol: Vol, 298 K). The ^{1}H NMR spectra of **L1** recorded at different pH values shows that protonation of **L1** to give [H**L1**]$^+$ species, occurring below pH 8, induces a marked downfield shift of the signal of the CH_2 group 3_{AL}, adjacent to the central nitrogen and to a minor shift for methylene 2_{AL}, suggesting that the first protonation step occurs on the central amine of the aliphatic chain. Further pH decrease below pH 6 and consequent formation of the [H_2**L1**]$^{2+}$ species induces a remarkable downfield shift of the signal of the CH_2 2_{AL} and negligible shift for the CH_2 3_{AL}, indicating that in [H_2**L1**]$^{2+}$ the two ammonium groups are localized on the two lateral benzylic amine groups, thus achieving a minimization of the repulsion between positive charges. Similarly, the pH dependence of the ^{1}H NMR signals of the CH_2 groups 2_{AL} and 4_{AL} of **L2** accounts for protonation of the central nitrogen in the [H**L2**]$^+$ species and of both benzylic amines in [H_2**L2**]$^+$.

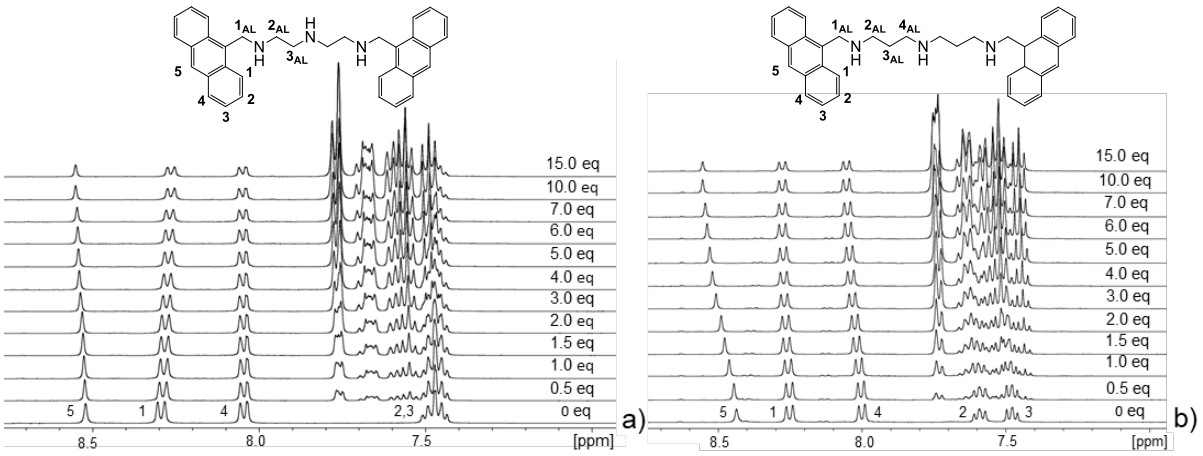

Figure S28. Aromatic signals of the ^{1}H NMR spectra of **L1** (a) and **L2** (b) at pH 7 D_2O/CD_3OD 30:70 (Vol:Vol) in the presence of increasing amounts of ketoprofen at 298 K. a) $J_{1,2}$ = 9 Hz, $J_{3,4}$ = 8 Hz. b) $J_{1,2}$ = 9 Hz, $J_{2,3}$ = 8 Hz, $J_{3,4}$ = 8 Hz.

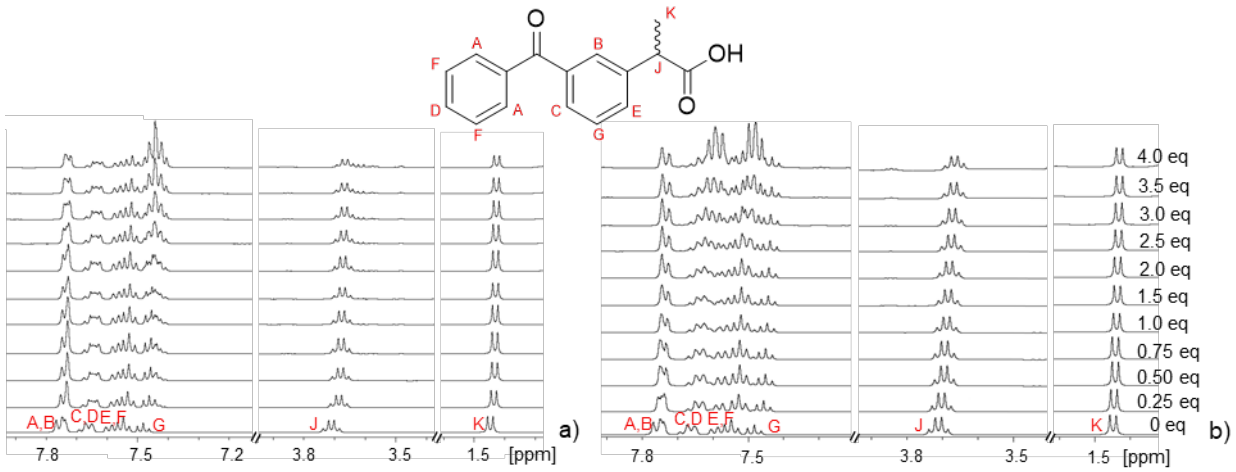

Figure S29. ^{1}H NMR spectra of ketoprofen at pH 7 D_2O/CD_3OD 30:70 (Vol:Vol) in the presence of increasing amounts of **L1** (a) and **L2** (b) at 298 K. $J_{J,K}$ = 7 Hz; the coupling constants values of the aromatic signals cannot confidently be determined due to signal superimposition.

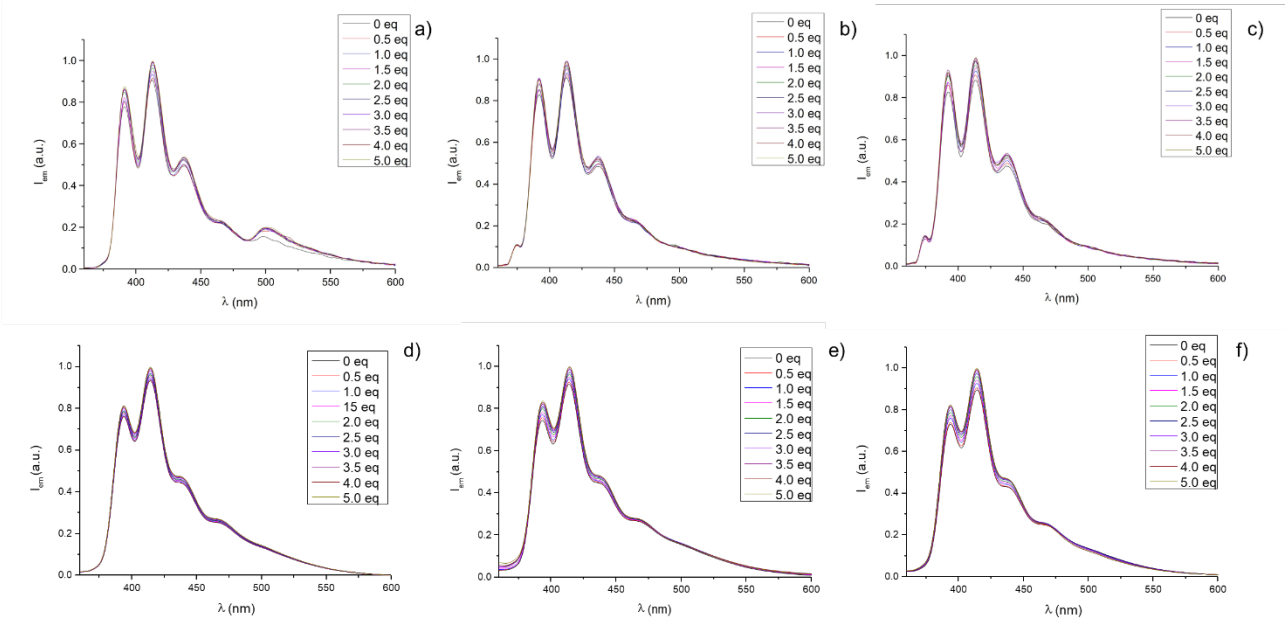

Figure S30. Emission spectra of **L1** and **L2** at pH 7 (0.001 M TRIS buffer, 298 K) in H_2O/EtOH 50:50 (Vol/Vol) in the presence of increasing amounts of sodium acetate ((a) **L1** and (d) **L2**), benzoic acid ((b) **L1** and (e) **L2**) and ibuprofen sodium salt ((c) **L1** and (f) **L2**). ([**L1**] = $1 \cdot 10^{-5}$ M, [**L2**] = $1 \cdot 10^{-5}$ M λ_{exc} = 340 nm).

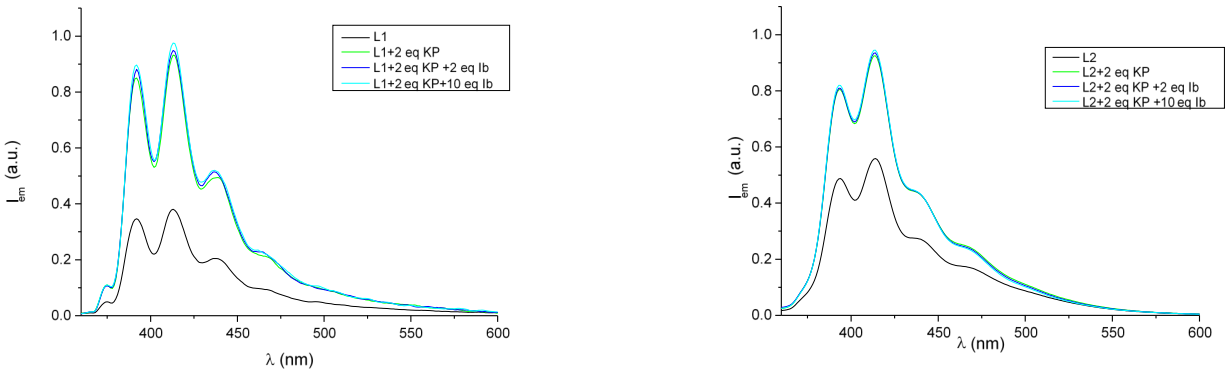

Figure S31. (a) Emission spectra of **L1** at pH 7 (0.001 M TRIS buffer, 298 K) in H_2O/EtOH 50:50 (Vol/Vol) in the absence (black line) and in the presence of KP only (2 equivs, green line) and KP (2 equivs) + ibuprofen (2 equivs, blu line or 10 equivs, cyan line) ([**L1**] = 10^{-5} M, λ_{exc} = 340 nm); emission spectra of **L2** at pH 7 (0.001 M TRIS buffer) in H_2O/EtOH 50:50 (Vol/Vol) in the absence (black line) and in the presence of KP only (2 equivs, green line) and KP (2 equivs) + ibuprofen (2 equivs, blu line or 10 equivs, cyan line) ([**L2**] = 10^{-5} M, λ_{exc} = 340 nm)

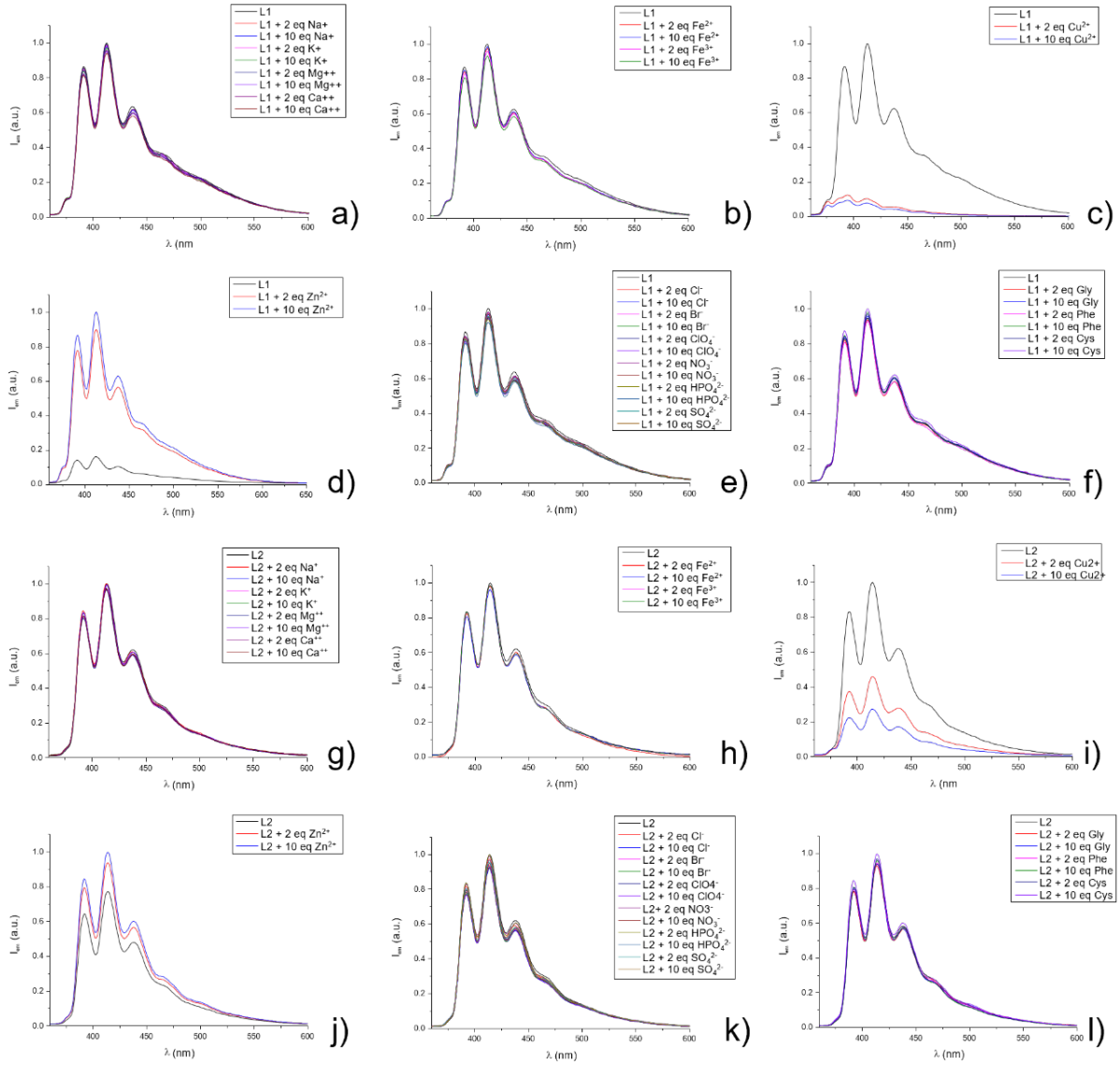

Figure S32. Emission spectra of **L1** (a-f) and **L2** (g-l) at pH 7 (0.001 M TRIS buffer, 298 K) in H_2O/EtOH 50:50 (Vol/Vol) in the absence and in the presence of 2 and 10 equivs. of different interfering agents. ([**L1**] = 10^{-5} M, [**L2**] = 10^{-5} M, λ_{exc} = 340 nm); a) **L1** + Na^+, K^+, Mg^{2+} or Ca^{2+} ; b) **L1** + Fe^{2+} or Fe^{3+}; c) **L1** + Cu^{2+}; d) **L1** + Zn^{2+}; e) **L1** + Cl^-, Br^-, ClO_4^-, NO_3^-, HPO_4^{2-} or SO_4^{2-}; f) **L1** + Gly, Phe or Cys; g) **L2** + Na^+, K^+, Mg^{2+} or Ca^{2+} ; h) **L2** + Fe^{2+} or Fe^{3+}; i) **L2** + Cu^{2+}; j) **L2** + Zn^{2+}; k) **L2** + Cl^-, Br^-, ClO_4^-, NO_3^-, HPO_4^{2-} or SO_4^{2-}; l) **L2** + Gly, Phe or Cys (pH 7, 0.001 M TRIS buffer, 298 K, H_2O/EtOH 50:50 (Vol/Vol)). The pH of the buffer was generally adjusted at 7 by addition of NaOH to a solution of TRIS·HCl. In the test with Na^+ as interfering agent the TRIS buffer at pH 7 was prepared starting form a TRIS·HCl solution and adjusting the pH at 7 with NMe_4OH, to avoid the presence of Na^+ in the tested solution; in the test with Cl^- as interfering agent the TRIS buffer at pH 7 was prepared by using TRIS free base and adjusting the pH at 7 with CF_3SO_3H, to avoid the presence of Cl^- in the tested solution.

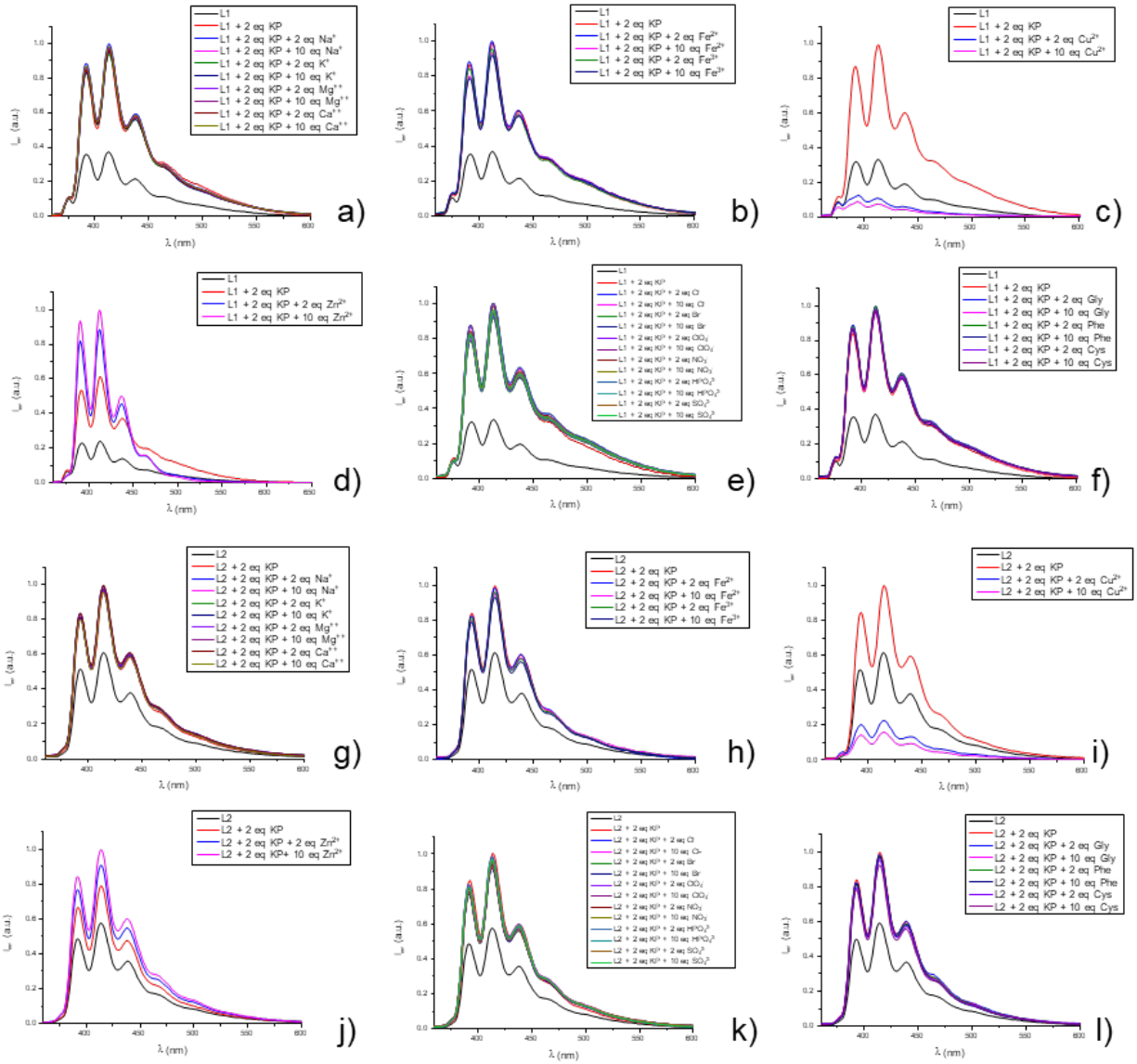

Figure S33. Emission spectra of **L1, L1** with 2 equivs. of KP and **L1** with 2 equivs. of KP in the presence of 2 and 10 equivs. of different interfering agents (a-f); emission spectra of **L2**, **L2** with 2 equivs. of KP and **L2** with 2 equivs. of KP in the presence of 2 and 10 equivs. of interfering agents. (pH 7, 0.001 M TRIS buffer, 298 K, in H_2O/EtOH 50:50 (Vol:Vol), [**L1**] = 10^{-5} M, [**L2**] = 10^{-5} M, λ_{exc} = 340 nm). a) **L1** + KP and Na^+, K^+, Mg^{2+} or Ca^{2+} ; b) **L1** + KP and Fe^{2+} or Fe^{3+}; c) **L1** + KP and Cu^{2+}; d) **L1** + KP and Zn^{2+}; e) **L1** + KP and Cl^-, Br^-, ClO_4^-, NO_3^-, HPO_4^{2-} or SO_4^{2-}; f) **L1** + KP and Gly, Phe or Cys; g) **L2** + KP and Na^+, K^+, Mg^{2+} or Ca^{2+} ; h) **L2** + KP and Fe^{2+} or Fe^{3+}; i) **L2** + KP and Cu^{2+}; j) **L2** + KP and Zn^{2+}; k) **L2** + KP and Cl^-, Br^-, ClO_4^-, NO_3^-, HPO_4^{2-} or SO_4^{2-}; l) **L2** + KP and Gly, Phe or Cys. (pH 7, 0.001 M TRIS buffer, 298 K, H_2O/EtOH 50:50 (Vol/Vol)). The pH of the buffer was generally adjusted at 7 by addition of NaOH to a solution of TRIS·HCl. In the test with Na^+ as interfering agent the TRIS buffer at pH 7 was prepared starting form a TRIS·HCl solution and adjusting the pH at 7 with NMe_4OH, to avoid the presence of Na^+ in the tested solution; in the test with Cl^- as interfering agent the TRIS buffer at pH 7 was prepared by using TRIS free base and adjusting the pH at 7 with CF_3SO_3H, to avoid the presence of Cl^- in the tested solution.

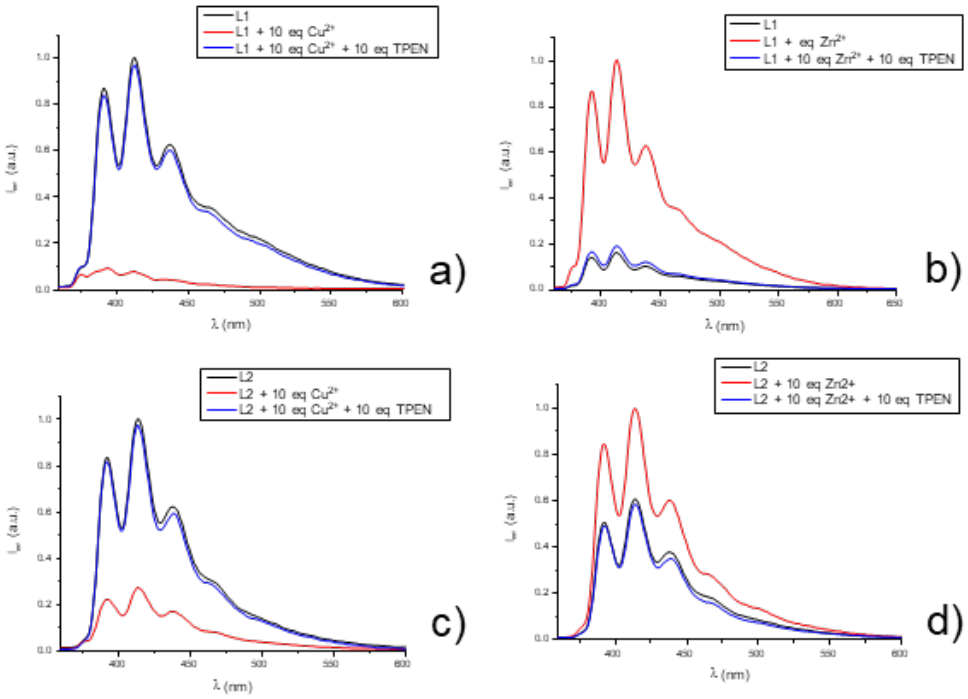

Figure S34. Effect of the addition of the metal chelator N,N,N',N'-tetrakis(2-pyridylmethyl)ethylenediamine (TPEN, 10 equivs) on solutions containing **L1** (a, b) and **L2** (c, d) and 10 equivs of Cu^{2+} and Zn^{2+}, displaying the restoral of original emission of both **L1** and **L2** upon addition of the metal sequestering agent TPEN (pH 7, 0.001 M TRIS buffer, 298 K, H_2O/EtOH 50:50 (Vol/Vol));

a) emission spectra of **L1**, **L1** in the presence of Cu^{2+} and **L1** in the presence of Cu^{2+} after the addition of TPEN;

b) emission spectra of **L1**, **L1** in the presence of Zn^{2+} and **L1** in the presence of Zn^{2+} after the addition of TPEN;

c) emission spectra of **L2**, **L2** in the presence of Cu^{2+} and **L2** in the presence of Cu^{2+} after the addition of TPEN;

d) emission spectra of **L2**, **L2** in the presence of Zn^{2+} and **L2** in the presence of Zn^{2+} after the addition of TPEN.

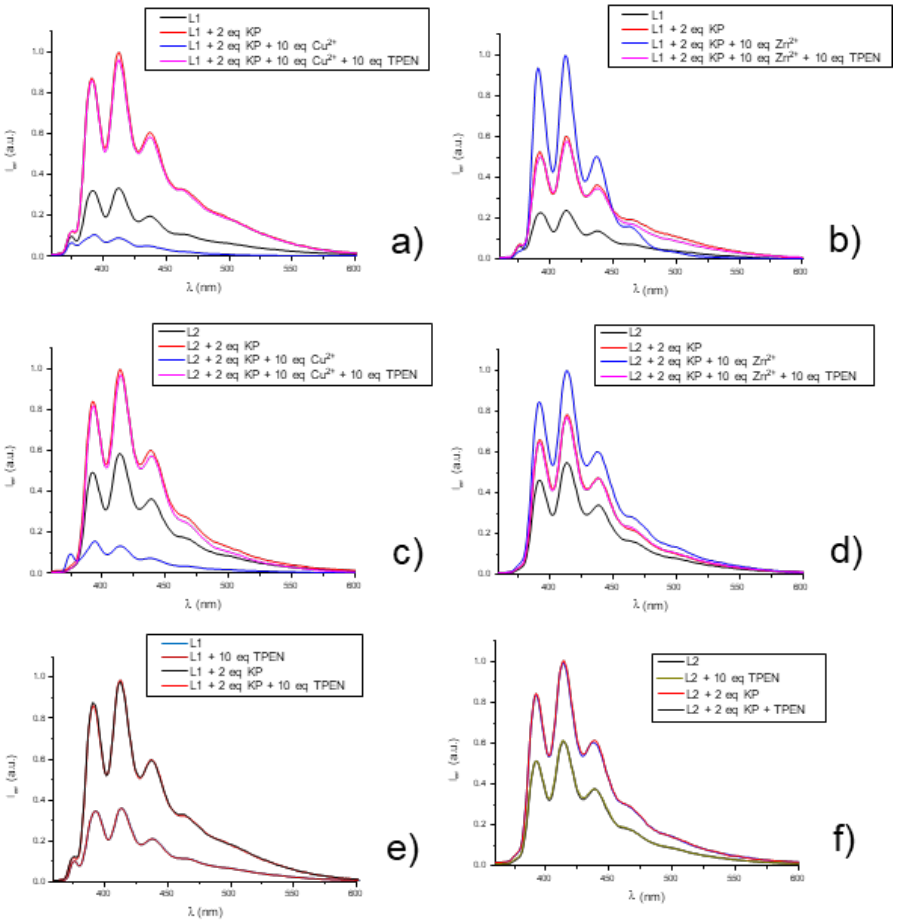

Figure S35. Effect of the addition of the metal chelator N,N,N',N'-tetrakis(2-pyridylmethyl)ethylenediamine (TPEN, 10 equivs) on solutions containing **L1** (a, b) and **L2** (c, d) in the presence of KP (2 equivs.) and added with 10 equivs of Cu^{2+} and Zn^{2+}, displaying the restoral of original emission of the KP complexes with **L1** and **L2** upon addition of the metal sequestering agent TPEN; the effect of the addition TPEN (10 equivs) to solutions containing **L1** or **L2** in the absence and in the absence of KP are also shown (e, f), to verify the absence of any interference of TPEN of the emission of **L1**, **L2** and their complexes (pH 7, 0.001 M TRIS buffer, 298 K, H_2O/EtOH 50:50 (Vol/Vol));

a) emission spectra of **L1**, **L1** in the presence of KP, **L1** in the presence of KP and Cu^{2+} and **L1** in the presence of KP, Cu^{2+} and EDTA;

b) emission spectra of **L1**, **L1** in the presence of KP, **L1** in the presence of KP and Zn^{2+} and **L1** in the presence of KP, Zn^{2+} and TPEN;

c) emission spectra of **L2**, **L2** in the presence of KP, **L2** in the presence of KP and Cu^{2+} and **L2** in the presence of KP, Cu^{2+} and TPEN;

d) emission spectra of **L2**, **L2** in the presence of KP, **L2** in the presence of KP and Zn^{2+} and **L1** in the presence of KP, Zn^{2+} and TPEN;

e) emission spectra of **L1**, **L1** in the presence of KP, **L1** in the presence of KP and TPEN and **L1** in the presence of KP and TPEN;

f) emission spectra of **L2**, **L2** in the presence of KP, **L2** in the presence of KP and TPEN and **L2** in the presence of KP and TPEN;

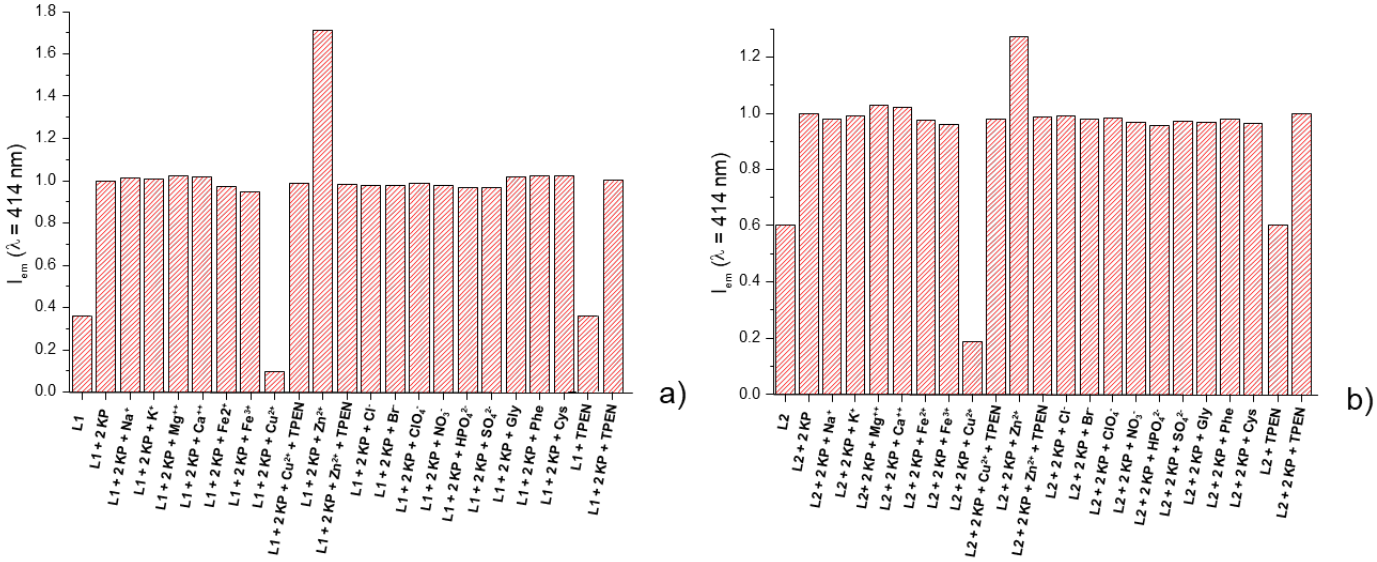

Figure S36. Emission intensity (a. u.) at 414 nm of **L1**, **L1** added with KP (2 equivs) and then treated with the different interfering agents tested (10 equivs.) (a) and of **L2, L2** added with KP (2 equivs) and then treated with the different interfering agents tested (10 equivs) (b). The emission intensity at 414 nm of **L1** and **L2** added of 2 equivs of KP and 10 equivs of N,N,N',N'-tetrakis(2-pyridylmethyl)ethylenediamine (TPEN) are also reported. Addition of TPEN does not influence the emission of **L1**, **L2** and their complexes with KP (pH 7, 0.001 M TRIS buffer, 298 K, H_2O/EtOH 50:50 (Vol/Vol)). All emission values have been referenced to those of **L1** (a) or **L2** in the presence of 2 equivs. of KP, whose values have been taken equal to 1.

Table S3. Crystallographic data and refinement parameters for compounds **1**.

	1
Formula	$(C_{36}H_{39}N_3)(C_{16}H_{13}O_3)_2 \cdot 0.75EtOH \cdot 2.75H_2O$
M	1101.55
T (K)	100
λ (Å)	1.54184
Crystal system, space group	Triclinic, P-1
Unit cell dimensions (Å, °)	a = 12.1823(3); α = 101.400(1) b = 13.0452(4); β = 99.006(1) c = 19.3857(5); γ = 101.858(1)
V ($Å^3$)	2892.5(1)
Z, ρ (mg/cm3)	2, 1.269
μ (mm^{-1})	0.666
F(000)	1184
Crystal size	0.20 X 0.22 X 0.27
θ range (°)	2.38 – 72.40
Reflns collected / unique (R_{int})	86439 / 11351 (0.0515)
Data / parameters	11351 / 769
Final R indices [I > 2σ]	R1 = 0.0631, wR2 = 0.1692
R indices (all data)	R1 = 0.0703, wR2 = 0.1763
GoF	1.012

Table S4. Selected torsion angles in **1**

H_2L2^{2+}	**Dihedral angle (°)**	**KP anions**	**Dihedral angle (°)**
C32-N1-C31-C17	68.1(2)	*S-enantiomer*	
C31-N1-C32-C33	-170.9(1)	τ1 = O1A-C10A-C8A-C9A	149.9(2)
C35-N2-C34-C33	-176.1(2)	τ2 = C2A-C3A-C7A-O3A	136.4(2)
C34-N2-C35-C36	179.7(2)	τ3 = C12A-C11A-C7A-O3A	-20.0(3)
C38-N3-C37-C36	173.6(2)	C1A-C6A / C11A/C16A[2]	59.99(7)
C37-N3-C38-C39	176.8(2)	*R-enantiomer*	
C17-C30 /C39-C52[1]	58.11(4)	τ1 = O1B-C10B-C8B-C9B	139.3(2)
		τ2 = C2B-C3B-C7B-O3B	-26.3(3)
		τ3 = C12B-C11B-C7B-O3B	-34.5(3)
		C1B-C6B / C11B-C16B[2]	56.34(8)

[1] = angle formed by the two mean planes defined by the carbon atoms of the two anthracene moieties

[2] = angle formed by the two mean planes defined by the carbon atoms of the two aromatic rings.

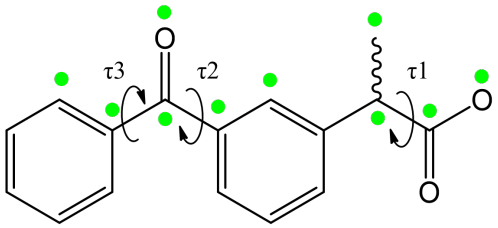

Scheme S2. Discussed torsion angles in KP anion.

Table S5. Torsion angles retrieved in the seven structures retrieved in the CSD.

CSD refcode	τ1 (°)	τ2 (°)	τ3 (°)
COZBAX[1]	96.3 / -83.4 / 175.6 / -69.3	16.4 / -34.2 / -18.7 / -21.6	42.1 / -28.8 / -47.5 / -32.5
KEMRUP	-128.2	21.7	31.5
KEMRUP01[2]	-132.3 / 152.4	20.2 / 16.7	31.5 / 38.7
MIRGAY[3]	139.6 / -81.6	-22.7 / 22.1	-26.6 / 26.7
MIRGAY01[3]	139.6 / -81.9	-22.7 / 22.1	-26.7 / 26.8
MIRGAY02	124.6 / -46.9	21.4 / -20.1	32.5 / -31.4
CCDC2012545[4]	-163.0 / -158.7	-22.1 / -30.9	-40.0 / -35.4

[1] = in the asymmetric unit of COZBAX four independent ketoprofen anion are present; [2] = in the asymmetric unit of KEMRUP01 two model for the disordered ketoprofen acid molecules are present; [3] = in the asymmetric unit of MIRGAY01 two independent ketoprofen acid molecules are present; [4] = in the asymmetric unit of CCDC2012545 two independent ketoprofen anion are present.

Table S6. Selected H-bond interactions in **1**.

D-H···A	D···A (Å)	H···A (Å)	D-H···A (°)
N1-H1N1···O3B	2.949(2)	2.18(3)	141(2)
N2-H1N2···O1A	2.664(2)	1.78(3)	158(3)
N2-H2N2···O1B	2.669(2)	1.79(3)	162(3)
N3-H2N3···O2A[1]	2.716(2)	1.79(2)	169(2)
N3-H1N3···O1B[1]	2.785(2)	1.84(3)	167(2)

[1] =-x+1,-y+1,-z+1

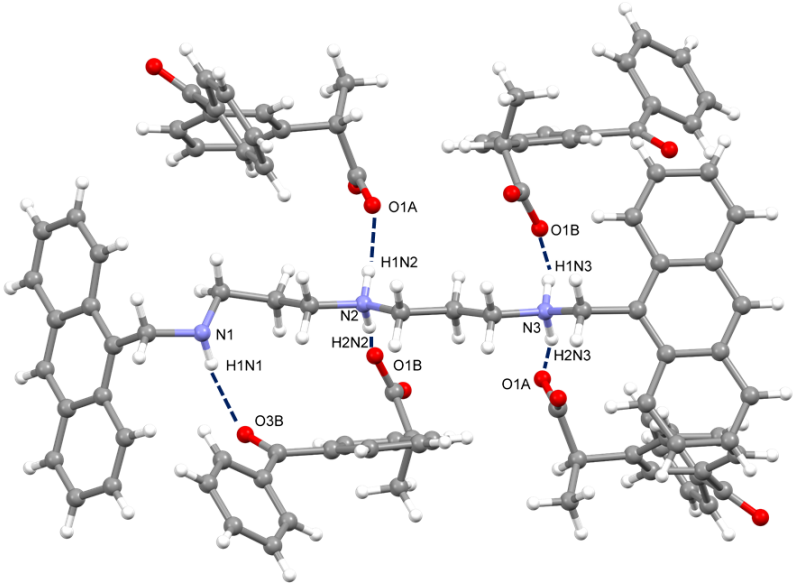

Figure S37. H-bonds scheme in **1**.

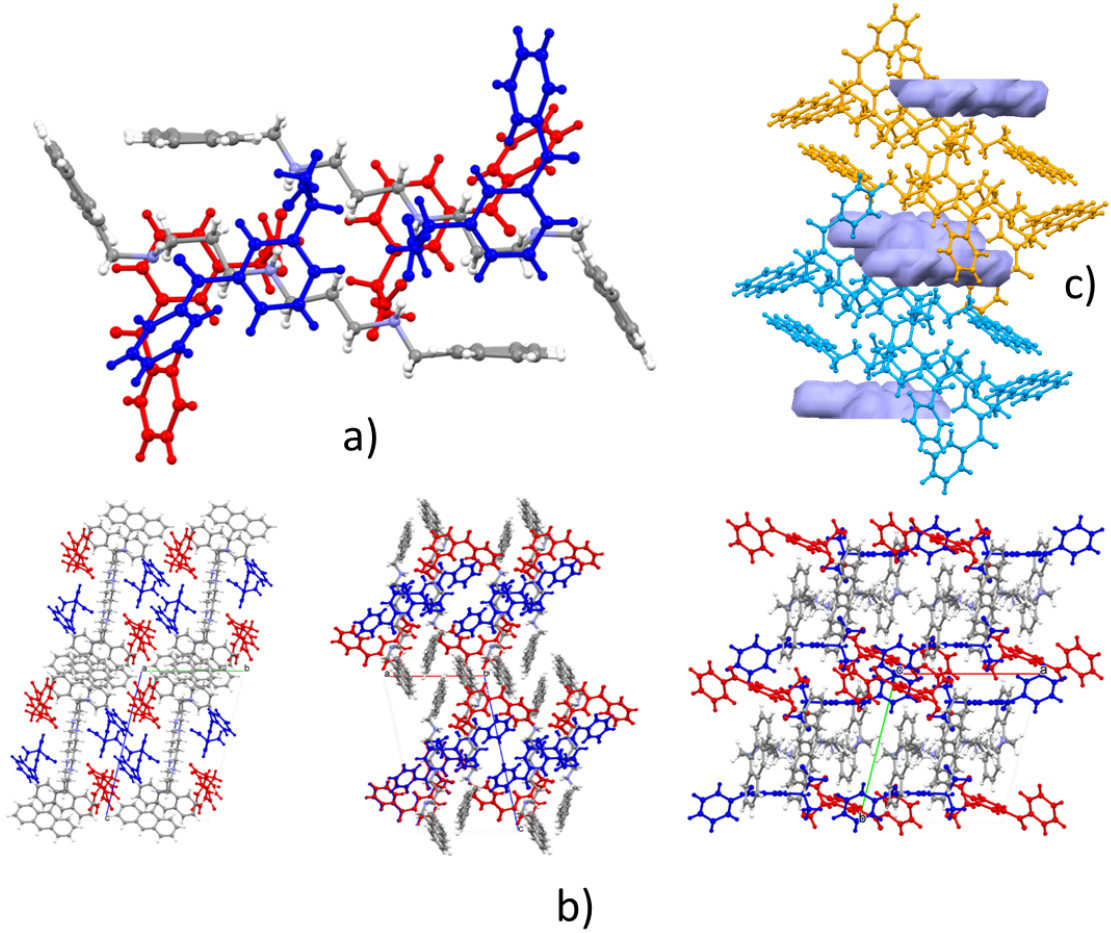

Figure S38. a) Disposition of KP anions in the 2:4 complex. R enantiomers, red, S enantiomers, blue. b) Disposition of the 2:4 complexes in the crystal packing of **1**, view along the a (left), b (middle) and c (right) axes. The colour scheme is the same of Figure S19 a). c) Spatial localization and volume (violet)occupied by solvent molecules (H_2O/EtOH). Packing is seen along the b axes.

REFERENCES

1. M. Savastano, C. Bazzicalupi, C. García-Gallarín, M. D. L. de la Torre, A. Bianchi and M. Melguizo, Supramolecular forces and their interplay in stabilizing complexes of organic anions: tuning binding selectivity in water, *Org. Chem. Front.*, 2018, **6**, 75–86.
2. Fontanelli, M.; Micheloni, M. *Proceedings of the I Spanish-Italian Congress on Thermodynamics of Metal Complexes*; Diputación de Castellón: Castellón, Spain, 1990; pp. 41–43.
3. M. Savastano, M. Fiaschi, G. Ferraro, P. Gratteri, P. Mariani, A. Bianchi and C. Bazzicalupi, *Sensing Zn^{2+} in Aqueous Solution with a Fluorescent Scorpiand Macrocyclic Ligand Decorated with an Anthracene Bearing Tail*, Molecules, 2020, 25, 1355.
4. G. Gran, Determination of the equivalence point in potentiometric titrations. Part II, *Analyst*, 1952, **77**, 661–671.
5. P. Gans, A. Sabatini and A. Vacca, Investigation of equilibria in solution. Determination of equilibrium constants with the HYPERQUAD suite of programs, *Talanta*, 1996, **43**, 1739–1753.
6. Mei, Q.; Shi, Y.; Hua Q.; Tong B. *RSC Adv.*, **2015**, 5, 74924-74931.
7. Bruker (2012). Bruker *APEX2*. Bruker AXS Inc., Madison, Wisconsin, USA.
8. Bruker (2012). Bruker *SAINT*. Bruker AXS Inc., Madison, Wisconsin, USA.
9. Krause, L.; Herbst-Irmer, R.; Sheldrick G.M.; Stalke D. *J. Appl. Cryst.,* **2015**, *48*, 3-10.
10. Burla, M. C.; Caliandro, R.; Camalli, M.; Carrozzini, B.; Cascarano, G. L.; Da Caro, L.; Giacovazzo, C.; Polidori, G.; Spagna, R., *J. Appl. Crystallogr.*,**2005**, 38, 381-388.
11. Sheldrick, G. M., *Acta Crystallogr., Sect. C: Struct. Chem.*,**2015**,71,3-8.
12. M. Nardelli, *J. Appl. Crystallogr.* **1995**, 28, 659.
13. C. F. Macrae, I. J. Bruno, J. A. Chisholm, P. R. Edgington, P. McCabe, E. Pidcock, E. Rodriguez-Monge, R. Taylor, J. van de Streek, P. A. Wood, *J. Appl. Crystallogr.* **2008**, *41*, 466-470.
14. Dassault Systèmes BIOVIA, Discovery Visualizer, v19.1.0.18287 (2019), San Diego: Dassault Systèmes.
15. P.Rossi, Paola Paoli, L.Chelazzi, S.Milazzo, D.Biagi, M.Valleri, A.Ienco, B.Valtancoli, L.Conti, *Cryst.Growth Des.* (2019), **20**, 226 (**COZBAX**)
16. P.Briard, J.C.Rossi, *Acta Crystallogr.,Sect.C:Cryst.Struct.Commun.* (1990), **46**, 1036. (**KEMRUP**)
17. S.Pawledzio, A.Makal, D.Trzybinski, K.Wozniak, *IUCrJ* (2018), **5**, 841 (**KEMRUP01**, **MIRGAY** and **MIRGAY01**)
18. P. Rossi, P. Paoli, A. Ienco, D. Biagi, M. Valleri, L. Conti, *Acta Cryst C*, **2019**, *75*, 783-792 (**MIRGAY02**)
19. P. Rossi, P. Paoli, S. Milazzo, L. Chelazzi, M. P. Giovannoni, G. Guerrini, A. Ienco, M. Valleri, L. Conti, *Crystals*, **2020**, *10*, 659-673. (**CCDC2012545**)
20. C. R. Groom, I. J. Bruno, M. P. Lightfoot and S. C. Ward, *Acta Cryst.,* **2016**, *B72*, 171-179.